

14

Microwaves in Photochemistry and Photocatalysis

Vladimír Církva

14.1

Introduction

Photochemistry is an interdisciplinary field pertaining to all natural sciences and many technical disciplines [1]. Many synthetic chemists retreat from using key photochemical steps [2] that might substantially reduce the number of reaction steps required to synthesize a desired product: photochemistry often achieves what ground-state chemistry cannot. Unfortunately, photoinduced reactions are only slowly being accepted by the synthetic organic community (only about 1% of the procedures in *Organic Syntheses* and *Organic Reactions* involve photochemical transformations) [3]. Two reasons are apparent: the course of photochemical reactions can be predicted only with difficulty, and the reactions are carried out using specific laboratory tools and devices.

Microwave (MW) radiation is a non-classical energy source, with photoactivation, ultrasound, high pressure, mechanical activation, supercritical fluids, electrochemistry, or plasma discharge. MW activation increases the efficiency of many processes and can simultaneously reduce the formation of the by-products obtained from conventionally heated reactions. Since the first reports of the use of MW heating to accelerate organic chemical transformations [4], numerous articles and books have been published on the subject of MW-assisted synthesis and related topics. MW chemistry has certainly become an important field of modern organic chemistry [5–9]. Chemical processes performed under the action of MW radiation are believed to be affected in part by superheating, hot-spot formation, and polarization [10]. The existence of a specific nonthermal MW effect has been a matter of controversy during recent years [5, 11].

In the past decade, the researchers have combined the action of ultraviolet/visible (UV/Vis) light on chemical substances with that of MW radiation to study possible synergic effects. Such a coupled activation is covered by the disciplines called *microwave photochemistry* and *microwave photocatalysis*. The energy of MW radiation (e.g., $E = 0.98 \text{ J mol}^{-1}$ at $\nu = 2.45 \text{ GHz}$) is considerably lower than that of UV/Vis radiation ($E = 600\text{--}170 \text{ kJ mol}^{-1}$ at $\lambda = 200\text{--}700 \text{ nm}$), thus insufficient to disrupt the bonds of common organic molecules. Therefore, we can assume that

UV/Vis radiation is responsible for a photochemical change, and MW radiation subsequently affects the course of the subsequent reaction [12].

MW chemistry has also been utilized in combination with some other unconventional activation processes. Such a connection might have a synergic effect on reaction efficiencies or, at least, enhance them by summing up the individual effects. Applications of MW radiation to ultrasound-assisted chemical [13] and electrochemical [14] processes have recently been described. The first comprehensive review on MWs in photochemistry was presented by Klán and Církva in the previous edition [12], and it covered the literature up to 2006. It provided the necessary theoretical background and some details about synthetic, analytical, environmental, and technical applications. A more recent review covering the literature up to 2009 was written by Církva and Relich [15]. Církva and Zabova published two reviews dedicated to thin TiO₂ films on an electrodeless discharge lamp (EDL) [16]. It demonstrated the outstanding improvements in degradative efficiency in MW photocatalysis. Another review, by Horikoshi and co-workers, dealt with the application of EDLs in advanced oxidation processes (AOPs) in the photocatalytic environmental remediation of pollutants [Rhodamine-B (RhB), 2,4-D, bisphenol-A, acetaldehyde, toluene, and dioxins] [17]. The current status of MW-assisted photochemical and photocatalytic applications in wastewater treatment was elaborated by Remya and Lin [18].

This chapter surveys the theory of the MW discharge in EDLs, their construction and spectral characteristics, preparation of titania-coated films, and their performance. Novel MW-assisted photochemical and photocatalytic reactors with different arrangements of the lamps in batch and flow-through experimental setups are described. The interactions of UV/Vis and MW radiation with matter are also discussed. The photochemical and photocatalytic reactions in batch and flow-through modes presented are summarized in several tables. Finally, some analytical, environmental, and other applications of EDLs are discussed.

14.2

UV/Vis Discharges in Electrodeless Lamps

The objective of MW-assisted photochemistry and photocatalysis is frequently, but not necessarily, connected with the EDL as a novel light source which generates UV/Vis radiation efficiently when placed in an MW field [12].

The EDL [19] consists of a glass envelope tube filled with an inert gas and an excitable substance and it is sealed under a low pressure. The MW field can trigger a gas discharge, causing the emission of UV/Vis radiation. This phenomenon has been studied for many years and was well understood in the 1960s [20]. The term “*electrodeless*” means that the lamps lack the electrodes within the envelope and as such the EDLs may be easily shaped depending on the application. The history of the scientific development and practical application of high-frequency EDLs as an optical spectral source goes back to the 1930s [21]. Jackson [22] began to use the radiation of a discharge to study the hyperfine structure of the cesium, indium,

and rubidium lines. A similar design of the spectral source was used by Meggers and Westfall [23] to excite various elements, such as the mercury isotope ^{198}Hg , the emission wavelength of which served as the ultimate standard of length.

However, such light sources have not been widely used because of technical difficulties connected with the application of a high-frequency field (i.e., MWs), and the lack of availability of pure noble gases and metals. The EDL is usually characterized by a higher emission intensity than that of hollow-cathode lamps, lower contamination, because of the absence of the electrodes, and a longer lifetime [24]. These lamps have been used in various applications as light sources and in atomic spectrometers.

14.2.1

Theory of Plasma-Chemical Microwave Discharges

Plasma is an ionized gas, a distinct fourth state of matter. “Ionized” means that at least one electron is not bound to an atom, converting the atoms into positively charged ions, which make plasma electrically conductive, internally interactive, and strongly responsive to an MW field [25].

The theory of Hg-EDL operation is shown in Figure 14.1. Free electrons in the fill (i.e., electrons that have become separated from the environment because of the ambient energy) accelerate as a result of the MW field energy [12]. They collide

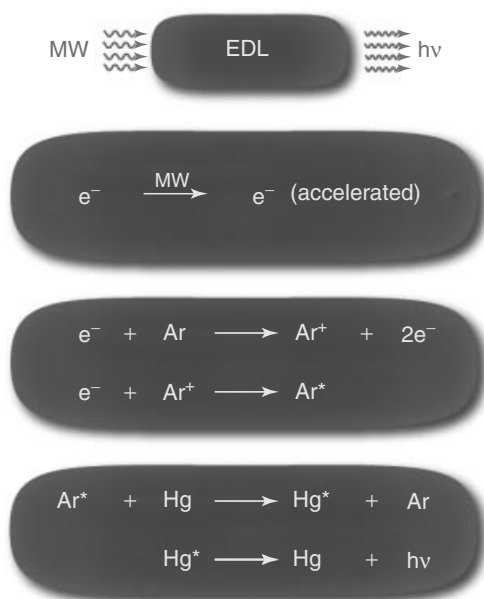


Figure 14.1 Principle of Hg-EDL operation and the release of emission energy as UV/Vis radiation in the Hg-EDL.

with argon atoms and ionize them to release more electrons. The repetitive effect causes the number of electrons to increase significantly over a short period of time, an effect known as an “*avalanche*.” The energetic electrons collide with the heavy-atom particles (argon or mercury) present in the plasma, exciting them from the ground state to higher energy levels. The excitation energy is then released as UV/Vis radiation with spectral characteristics that depend on the composition of the envelope. The excited molecular or atomic species in the plasma can emit photons over a very broad portion of the electromagnetic spectrum, ranging from X-rays to the IR region [26].

14.2.2

Construction of MW-Powered EDLs

The EDL system is modular and consists of two basic parts, a gas-filled bulb and an MW power supply with magnetron. A typical EDL is made of a quartz or Pyrex tube envelope, which contains a noble gas and an excitable substance. The envelope material must be impermeable to gases, an electrical insulator, and chemically resistant to the filling compounds at the temperature of operation.

The construction of MW-excited EDLs is relatively straightforward but there are a number of operating parameters in their preparation that have to be considered in order to produce an intense light source. The desired characteristics and requirements for EDLs are high intensity, great stability, long lifetime, and, to a lesser extent, low cost and high versatility. In practice, it is very difficult to meet all of these desired characteristics simultaneously.

General procedures for EDL construction are available in the literature [27–29]. However, many minor details, which are critical for the proper functioning of the lamp, are often omitted. The investigator who wants to make an EDL is thus faced with a very large amount of information dispersed in the literature, and finds that it is very difficult to reproduce these procedures to develop EDLs having desired properties. An experimental vacuum system for construction of an EDL (Hg, HgI₂, Cd, I₂, KI, P, Se, and S) was recently designed by Církva *et al.* (Figure 14.2) [30]. The Pyrex EDL blank envelope was cleaned in a water–soap mixture, and then washed with distilled water, aqueous 10% hydrofluoric acid, and ethanol. Hg (2.5 μl) and a stainless-steel thin wire (3 cm) were placed in the EDL blank. The system was flushed with argon and sealed under 20 Torr (2.67 kPa) vacuum. This technique is very simple and enables EDLs to be prepared in a common chemical laboratory.

The length of the EDL was 50 mm (diameter 20-mm) and photographs of an Hg-EDL and an S-EDL are shown in Figure 14.3. Testing the EDL performance was carried out in order to prepare the lamps for spectral measurements [30]. A typical experimental system for such tests consisted of a round-bottomed flask containing *n*-heptane, equipped with a fiber-optic temperature and spectral probe, and a Dimroth condenser, and was placed in a MW oven (Figure 14.4).

Another novel environmental risk-free (Hg-free) EDL was constructed by Horikoshi *et al.* [31] using the device illustrated in Figure 14.5. A quartz ampoule (from Ichikawa Pressure Industrial) was connected to vacuum and was then

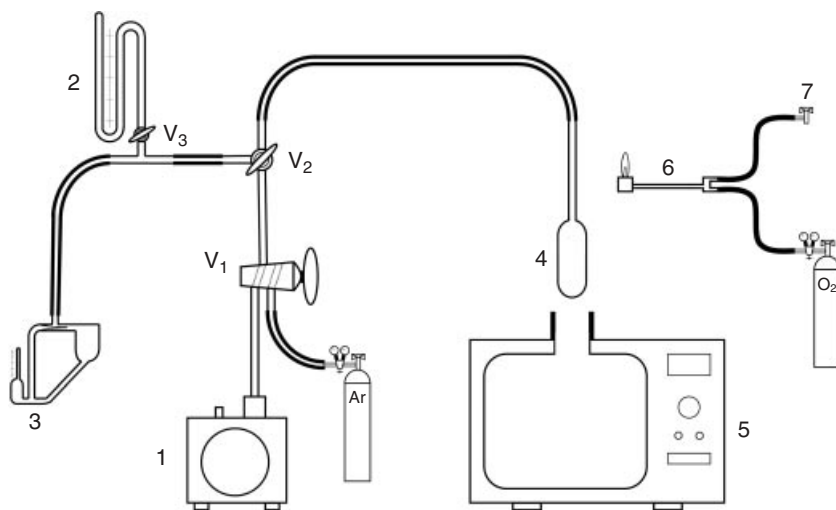


Figure 14.2 Vacuum system for manufacture of an EDL: (1) rotary vacuum pump, (2) mercury manometer, (3) tilting-type McLeod pressure gauge, (4) EDL blank, (5) modified MW oven, (6) glass-working burner, and (7) natural gas, V_1 – V_3 are stopcocks [30].

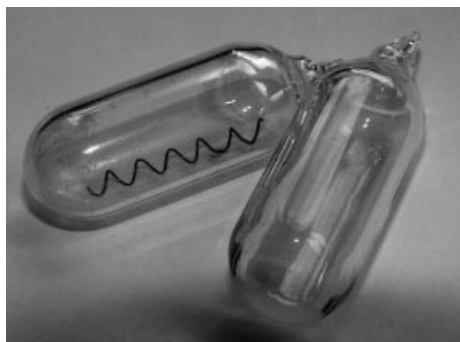


Figure 14.3 Hg-EDL and S-EDL for photochemical applications.

arranged in the MW waveguide. The EDL length was 145 mm (diameter 18 mm), the initial internal pressure was set at 10^{-3} Torr (0.133 Pa), and the target gas (He, Ar, Xe, H_2 , N_2 , O_2 , or a binary gas mixture thereof) was used. These EDLs were examined (under the optimized conditions) for using in AOPs (photoassisted or photocatalyzed degradations).

A novel Hg-free Dewar-like (double-walled structure) microwave discharge thermally insulated electrodeless lamp (MDTIEL) was fabricated by Horikoshi *et al.* [32]. The gas fill in the lamp was changed to the more eco-friendly N_2 gas. The lower temperature on the external surface should make it attractive in carrying out heat-sensitive photochemical reactions.



Figure 14.4 Testing the EDL performance in a Milestone MicroSYNTH Labstation [30].

14.2.3

Preparation of the Thin Titania Films on EDLs

Photocatalysis is an efficient, attractive, and clean technology for pollution abatement in water under mild conditions [33]. Titanium(IV) oxide (titania) is an archetypical photocatalytic material because it is endowed with an inherent photocatalytic activity. Moreover, it is inexpensive, very chemically and thermally stable, nontoxic, and available in large amounts [34]. For better recovery and reuse, titania can be prepared in immobilized form as a thin film on a glass substrate as a catalyst support. A major advantage here is that the reaction products and photocatalyst do not have to be separated, unlike when using powder or colloidal suspensions (slurries) of the photocatalyst [35]. However, the immobilized films produced by common sol-gel methods exhibit relatively low photocatalytic activity because of their low surface area and small film thickness. Also, TiO_2 is photoactive only

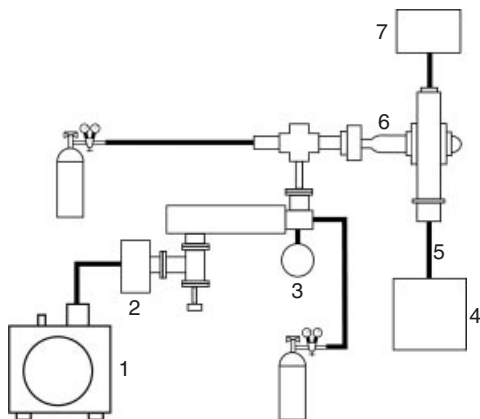


Figure 14.5 Experimental setup for the examination of optimized conditions in the EDL system: (1) rotary vacuum pump, (2) turbomolecular pump, (3) capacitance manometer, (4) MW generator, (5) MW coaxial cable, (6) EDL blank, and (7) UV/Vis spectrometer [31].

under UV/Vis irradiation with an adsorption edge wavelength of typically less than 388 nm (i.e., 3.2 eV bandgap). Likewise, the fast recombination rate (the mean e^-/h^+ lifetime is about 30 ns) of photoinduced electron–hole pairs leads to a low photoactivity of titania. Doping TiO_2 with transition metal ions [36] has frequently been attempted, not only to retard the fast charge pair recombination but also to permit visible light absorption by providing defect states in the bandgap.

The sol–gel route is one of the most successful techniques for preparing nanosized metallic oxide materials with high photocatalytic activities. By tailoring the chemical structure of the primary precursor and carefully controlling the processing variables, nanocrystalline products with very high levels of chemical purity can be produced [37]. In sol–gel processes, TiO_2 is usually prepared by the following reactions: hydrolysis and polycondensation of titanium alkoxides, $\text{Ti}(\text{OR})_4$ ($\text{R} = i\text{-Pr}, n\text{-Bu}$), to form oxopolymers, which are then transformed into an oxide network [38]. The overall reaction is usually written as $\text{Ti}(\text{OR})_4 + 2 \text{H}_2\text{O} \rightarrow \text{TiO}_2 + 4\text{ROH}$.

The condensation is usually accomplished by gel formation and calcination. The condensation pulls together the constituent particles of the gel into a compact mass, thus building up the metal oxide crystal. The calcination temperature is especially important for removing the organic molecules from the final products. The sol–gel-derived precipitates are amorphous in nature, requiring further heat treatment at a high temperature to induce crystallization.

The sol–gel method within templates of surfactant assemblies organized as reverse micelles is an effective strategy for the generation of uniform metal oxide nanoparticles finalized as thin films [39]. In this process, the alkoxide hydrolyzes inside a reverse micelle with a limited amount of water. Then the polycondensation step could proceed simultaneously and is highly competitive. Compared with other

methods, the surfactant-mediated sol–gel provides good control of the hydrolysis rate [40].

The titania photocatalyst on Hg-EDLs can be prepared using a sol–gel method:

- 1) **From titanium(IV) isopropoxide, $\text{Ti}(i\text{-PrO})_4$** [41]: The titania sol was prepared by hydrolysis of $\text{Ti}(i\text{-PrO})_4$ according to the method described by Kluson *et al.* [42]. The hydrolysis was carried out in the reverse micelles of Triton X-100 in cyclohexane. The molar ratios of the initial compounds were 1:1:1 [water:Triton X-100: $\text{Ti}(i\text{-PrO})_4$] and the Triton X-100:cyclohexane volume ratio was 0.45.
- 2) **From titanium(IV) butoxide, $\text{Ti}(n\text{-BuO})_4$** [43]: $\text{Ti}(n\text{-BuO})_4$ was dissolved in acetylacetone and ethanol in a volume ratio of 1:1:1. Then the water used for hydrolysis was added dropwise [the $\text{Ti}(n\text{-BuO})_4$:water molar ratio was 0.1] under mechanical stirring to form sol and gel.

As in the case of all surface-finishing techniques, it is also important to maintain a high level of surface cleanliness to ensure good adhesion between the substrate and the surface coating [41]. Prior to the film deposition, the support (EDL) was thoroughly cleaned in a water–soap mixture, rinsed with distilled water, soaked in a solution of HCl (1.0 mol l^{-1}), and rinsed with water and ethanol. In this method, the support is slowly dipped into and withdrawn from a tank containing the gel (using a dip-coating machine), with a uniform velocity (6 cm min^{-1}), in order to obtain a uniform coating. The films were then dried at room temperature for 1 h and finalized by thermal treatment at 500°C for 2 h (2°C min^{-1}) [41, 43] to form the titania-coated Hg-EDLs (Figure 14.6).

Titania-doped transition metal (M/TiO_2) thin films have also been prepared [43] by the sol–gel method using $\text{Ti}(n\text{-BuO})_4$ and transition metal acetylacetonates as precursors. For the preparation of M/TiO_2 sol, transition metal acetylacetonate (0.1–0.95 g) was dissolved in a 10 ml of acetylacetone, then $\text{Ti}(n\text{-BuO})_4$ was added followed by 0.1 ml of concentrated nitric acid and 10 ml of ethanol. Finally, 4 ml of water was added dropwise. In order to obtain a homogeneous mixture of M/TiO_2 , the solution was stirred vigorously for 2 h. Figure 14.7 shows the flow chart for the preparation of titania-doped transition metal thin films. Typical sols were prepared



Figure 14.6 Prepared titania-coated Hg-EDL.

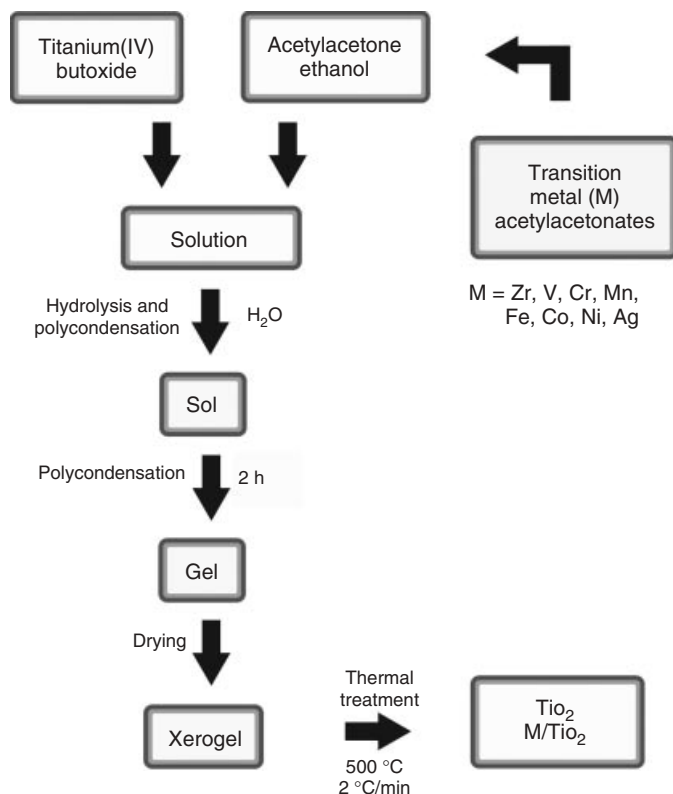


Figure 14.7 Flow chart for the sol-gel processing of titania-doped thin films [16, 43].

for various transition metals ($M = \text{Zr, V, Cr, Mn, Fe, Co, Ni, and Ag}$) [43] and various weight percentage concentrations of transition metal (1, 3, 5, and 9 wt%).

The prepared titania and titania-doped (M/TiO_2) thin films were characterized [16, 43] by several techniques: X-ray diffraction (XRD), Raman spectroscopy, X-ray photoelectron spectroscopy (XPS), scanning electron microscopy (SEM), atomic force microscopy (AFM), and UV/Vis absorption spectroscopy. Also, the photocatalytic activity of titania films was examined by the RhB decomposition test [16, 43].

14.2.4

Spectral Characteristics of the EDLs

Knowledge of the spectral characteristics of EDLs [44, 45] is clearly essential for planning MW-assisted photochemical and photocatalytic experiments. A suitable choice of the EDL envelope and fill material can be very useful in planning an efficient course of a photochemical or photocatalytic process without the need for filtering off the undesirable part of the UV/Vis radiation using other tools, such as glass, solution filters, or monochromators.

The total emission output of an Hg-EDL in the region of 200–700 nm is approximately the same as that of an electrode lamp with the same power input [46]. The distribution of radiation is, however, markedly different, as a result of a much higher Hg pressure and the greater number of atoms that are present in the plasma. An EDL emits over three times as much UV and over half as much IR radiation as a conventional lamp.

The spectral measurements were accomplished in an MW oven (such as that in Figure 14.4) described elsewhere [44], which had a window for UV/Vis radiation coming from the EDL to a spectrometer. Its power was adjusted to the maximum in order to guarantee continuous MW irradiation. Every liquid immediately boils since an EDL produces a considerable amount of IR radiation. Spectral measurements of prepared EDLs (light intensity in microwatts per square centimeter) were carried out on an AVS-S2000 spectrometer with an AvaSoft software package and a USB2000 spectrometer with an fiber-optic probe and an operating OOIrrad-C software package (Ocean Optics) [30, 44, 45].

Müller *et al.* [45] reported the emission characteristics of various EDLs containing different fill material (such as, Hg, HgI₂, Cd, I₂, KI, P, Se, or S) in the region of 250–650 nm. Whereas distinct line emission peaks were found for the mercury, cadmium, and phosphorus fills (Figure 14.8), the iodine-, selenium-, and sulfur-containing EDLs (Figure 14.8) emitted continuous bands. The sulfur-containing EDL has been proposed for assisting phototransformations that are of environmental interest because the emission flux is comparable to solar terrestrial radiation.

Another novel Hg-free EDL was developed by Horikoshi *et al.* [31] using only gases (He, Ar, Xe, H₂, N₂, O₂, or a binary gas mixture thereof). This EDL was optimized through examination of the light intensity at controlled pressures and gas mixture ratios. The most suitable EDL with lines concentrated in the 300–400 nm spectral range (296, 315, 336, 353, and 357 nm) was obtained with an N₂:Ar ratio of 20:80 by volume at a pressure of ~700 Pa.

In addition, the EDL spectra could easily be modified by choosing a suitable EDL envelope glass material, fill material, nature and pressure of the inert fill gas, temperature, MW output power, and solvent polarity according to the needs of a particular photochemical or photocatalytic experiment [44] (see also Section 14.2.5).

14.2.5

Performance of the EDLs

The performance of EDLs depends strongly on many preparation and operating parameters, such as envelope glass material, fill material, nature and pressure of the inert fill gas, EDL temperature, MW output power, and solvent polarity [47].

14.2.5.1 Effect of Envelope Material

High-quality quartz is the most widely used lamp envelope materials but early EDLs were manufactured used glass, Vycor, or Pyrex [27]. In addition, the envelope glass material filters off the part of the UV/Vis radiation from the EDL. Figure 14.9

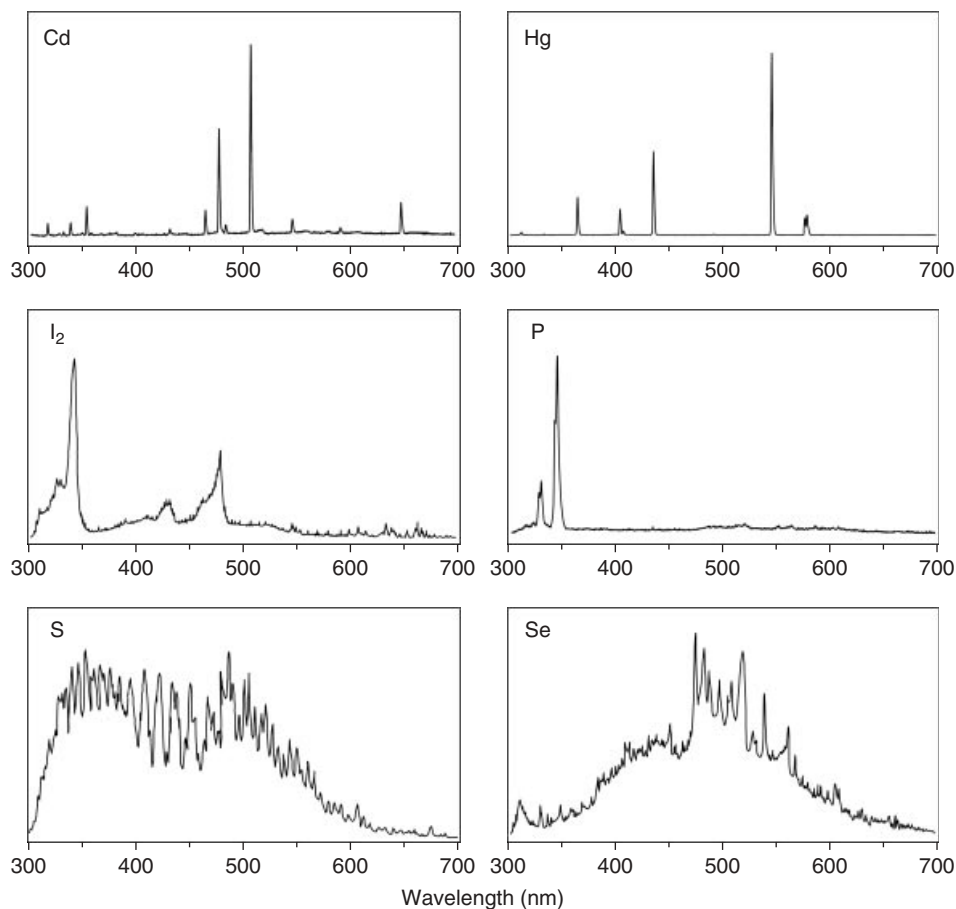


Figure 14.8 Emission spectra of Hg-, Cd-, I-, P-, S-, and Se-EDLs (Pyrex, 5 Torr of Ar) [30, 45].

shows a comparison of the emission spectra of quartz and Pyrex Hg-EDLs [44, 48]. The Pyrex glass completely removed the 254 and 297 nm bands; however, the intensity of the remaining bands was the same.

14.2.5.2 Effect of Fill Material

The choice of the fill material initiating the discharge is very important. Together with a standard mercury fill, it is often desirable to incorporate an additive in the fill material that has a low ionization potential and a sufficient vapor pressure (Cd, S, Se, Zn) [49, 50]. One category of low ionization-potential materials is the group of alkali metals or their halides (LiI, NaI), but some other elements, such as Al, Ga, In, Tl [51, 52], Be, Mg, Ca, Sr, La, Pr, or Nd [53–55], can also be used. Other metal-containing compounds have been utilized to prepare EDLs, including

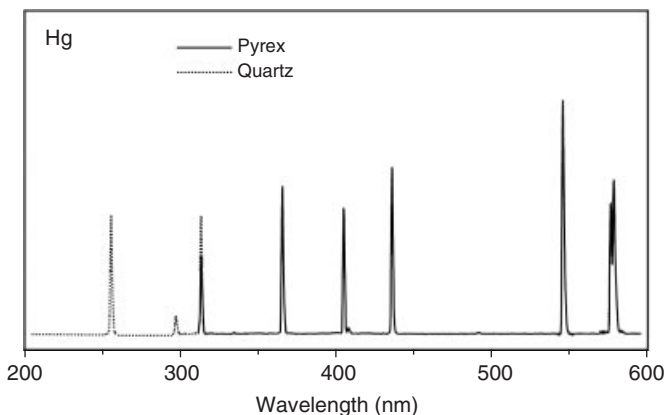


Figure 14.9 Emission spectra of quartz and Pyrex Hg-EDLs in hexane [44].

amalgams of Cd, Cu, Ag, and Zn. Multi-element EDLs have been prepared using combinations of elements (e.g., Li–Na–K, As–Sb, Co–Ni, Cr–Mn, Bi–Hg–Se–Te, Cd–Zn, Ga–In, and Se–Te) [56]. The spectral output from each individual element is very sensitive to temperature [57].

A combination of metal halides may be used to provide the desired characteristics, for example, AlX_3 , InX , and/or TlX (X =halide) [58] may be combined with one or more lanthanide halides (CeX_3 , GdX_3 , DyX_3 , HoX_3 , ErX_3). It has been found that no inter-element interferences occur in the lamp. The EDLs filled with a variety of compounds and the corresponding EDL emission wavelengths reported in the literature are summarized in Table 14.1.

14.2.5.3 Effect of Nature and Pressure of Inert Fill Gas

The arc chamber contains a buffer noble gas (usually Kr, Xe, or Ar) which is inert to the extent that it does not adversely affect the lamp operation. Helium has a higher thermal conductivity than other noble gases and, therefore, a higher thermal conduction loss is observed [53]. The inert gas easily ionizes at low pressure but its transition to the thermal arc is slower and the lamp requires a longer warm-up time. Ionization is more difficult at higher pressures and it requires a higher input power to establish the discharge.

In general, it has been recommended that the pressure of the filling gas should be maintained between 2 and 20 Torr (0.266–2.67 kPa); at the operating temperature it is usually much higher (10 atm) than that of a conventional electrode lamp. Utilizing argon was considered to be the best compromise between high EDL radiance and long lifetime. Air cannot be used, owing to the quenching properties in a MW plasma just like water vapor. To focus the MW field efficiently into the EDL, a special Cd low-pressure lamp with a metal antenna (molybdenum foil) was developed for experiments in MW-absorbing liquids [66].

The emission intensities of Hg-EDLs and S-EDLs have been scaled according to spectral area (300–450 nm) depending on the pressure of argon in the range

Table 14.1 Filling materials and the emission wavelengths of EDLs.

Filling material (inert gas)	Excited species	Emission wavelength, λ (nm)	Ref.
AlBr ₃ (Ne)	AlBr [*]	278	[59]
AlCl ₃ (Ne)	AlCl [*] , Al	261, 308, 394, 396	[60, 61]
Ar (Ar)	Ar ₂	126, 107–165, 812	[26, 62]
Br ₂ (Xe)	XeBr [*]	282	[63]
Br ₂ (Kr)	KrBr [*] , Br ₂ [*]	207, 291	[64]
Cd (Ar)	Cd	229, 327, 347, 361, 468, 480, 509, 644	[45, 65–70]
Cl ₂ (Ar)	ArCl [*]	175	[26, 62]
Cl ₂ (Xe)	XeCl [*]	308	[26, 62]
Cl ₂ (Kr)	KrCl [*]	222	[63]
CuCl (Ar)	Cu	325, 327	[65]
FeCl ₂ (Ar)	Fe	248, 272, 358, 372–376	[65]
GaI ₃ (Ar)	Ga	403, 417, 380–450	[71, 72]
Hg (Ar)	Hg	185, 254, 297, 313, 365, 405, 436, 546, 577, 579	[45, 65, 66, 71, 73–76]
HgI ₂ (Ar)	Hg, HgI [*]	Hg lines + 440	[45]
I ₂ (Ar)	I ₂ [*]	342	[45]
I ₂ (Xe)	XeI [*]	253	[63]
I ₂ (Kr)	I + I ₂ [*]	178, 180, 183, 184, 188, 206, 342	[64, 77–80]
InI ₃ (Ar)	In	410, 451	[72]
LaI ₃ (Ar)	La	Lines 240–290 nm	[81]
Mg, H ₂ (Ar)	MgH [*]	518, 521, 480–560	[82]
N ₂ (Ar)	N ₂	296, 315, 336, 353, 357	[31, 32]
NaI (Xe, Kr)	Na	589	[83, 84]
P (Ar)	P	325, 327, 343	[45]
S (Ar)	S	320–850, 525	[45, 51, 85–88]
Se (Ar, Xe)	Se	370–850, 545	[45, 86, 87, 89, 90]
SnI ₂ (Ar)	Sn	400–850, 610	[91, 92]
Te (Ar)	Te	390–850, 565	[86, 87, 90]
TlI (Ar)	Tl	277, 352, 378, 535	[65, 72]
Zn (Ar)	Zn	214, 330, 468	[65, 66, 72]
ZrI ₄ (Ar)	Zr	Lines 220–290 nm	[81]

0.1–20 Torr (13–2666 Pa) (Figure 14.10). Also, the effect of the spiral (resistance wire steel, tantalum) on the EDL intensity was studied [93]. The best results were obtained for an Hg-EDL with a pressure of 20 Torr (2.5 μ Hg, steel spiral) and for an S-EDL with a pressure of 0.1 Torr (5 μ g S, tantalum spiral).

The EDLs can be evaluated in the photochemical *cis-trans* photoisomerization of *trans*-stilbene (Figure 14.11). This method [93] makes it possible to compare the

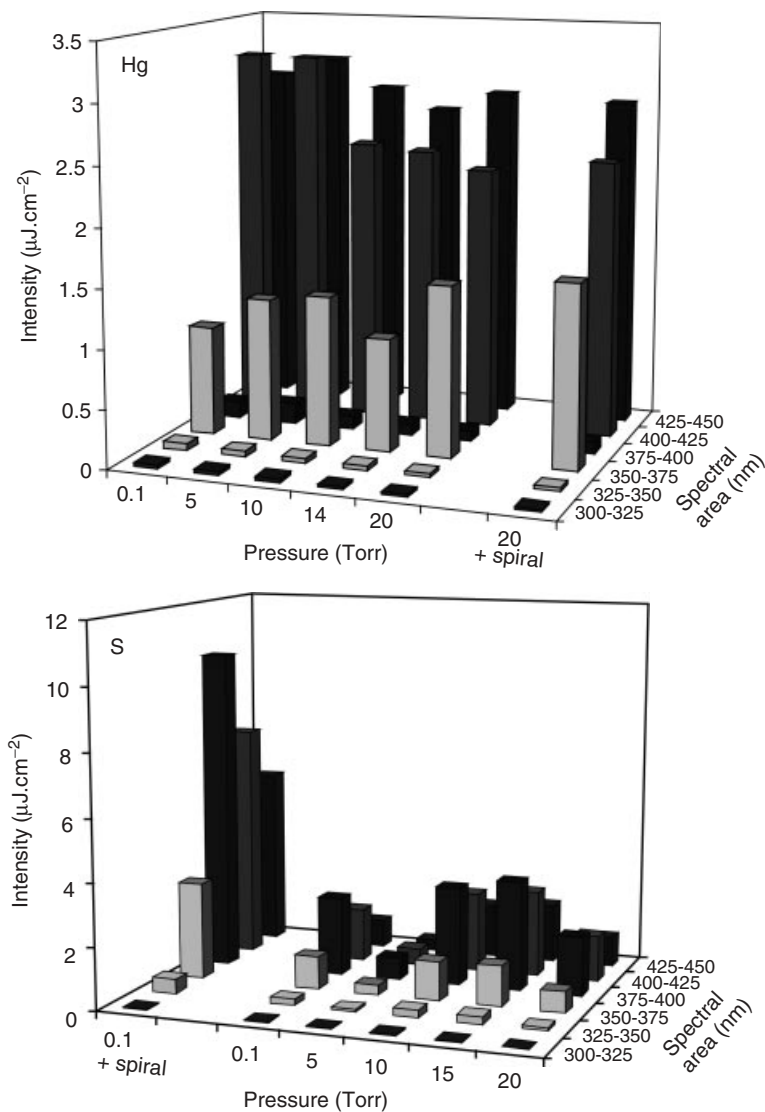


Figure 14.10 Dependence of the Hg-EDL and S-EDL intensity on the argon pressure according to spectral area [93].

different EDLs (Hg versus S) at different pressures (5 versus 20 Torr) and this is currently under investigation.

14.2.5.4 Effect of EDL Temperature

Operation at a high power or high temperature can increase the emission intensity but, at the same time, reduce the lamp lifetime and lead to broadening of the atomic line profile due to self-absorption and self-reversal effects. It was found

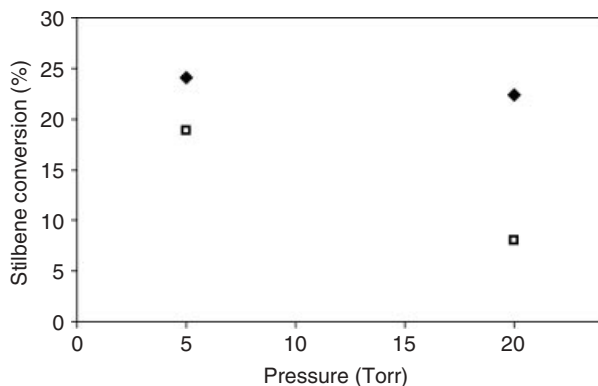


Figure 14.11 EDL evaluation on the photoisomerization of *trans*- to *cis*-stilbene (◆, Hg-EDL; □, S-EDL) [93].

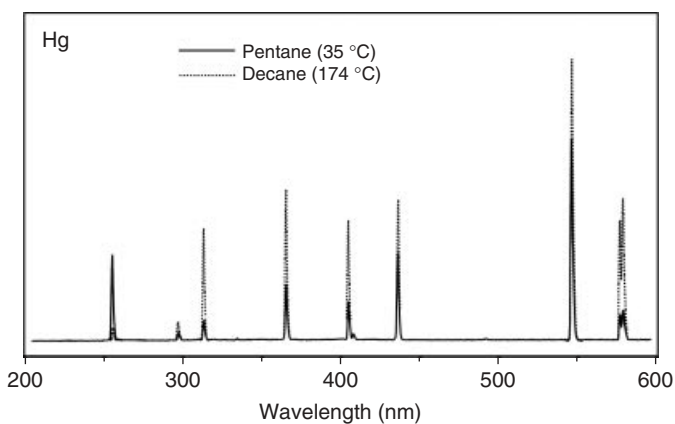


Figure 14.12 Emission spectra of a quartz Hg-EDL in pentane and decane [44].

that the optimum operating temperature for the mercury filling is 42 °C (for the 254 nm line, $6^1 S_0-6^3 P_1$) [65]. The output is reduced when the temperature is beyond the optimum [44].

The relative intensities of the mercury emission peaks in EDLs were found [44] to be very dependent on temperature (35–174 °C, in various hydrocarbons); the 254 nm short-wavelength band was suppressed with increase in temperature; however, the 366 nm line was enhanced (Figure 14.12).

14.2.5.5 Effect of Microwave Output Power

The frequency and intensity of electromagnetic energy are determined by the type of device used. MW energy is widely used for the excitation of EDLs because it is generally more efficient than radiofrequency energy for the generation of intense light. MW radiation for the excitation of gas discharges is usually generated by a fixed-frequency (2.45 GHz) magnetron oscillator. The effect of the MW reactor

output power on the relative peak intensities has also been investigated [44, 93] (Figure 14.13). It was found that the EDL intensity increased with increase in MW power (30 and 300 W).

14.2.5.6 Effect of Solvent Polarity

Solvents that absorb MW radiation significantly reduced the EDL intensities of all emission bands since it reduces the amount of MW energy that powers the lamp [44]. The EDL spectrum in methanol is compared with that in hexane in Figure 14.14. Likewise, the solvent can also be used as an internal UV filter; benzene significantly suppressed wavelengths below 280 nm. Therefore, hexane is ideal when a short-wavelength irradiation (254 nm) experiment is carried out. It can be concluded that the right choice of the EDL envelope material (quartz, Pyrex) and

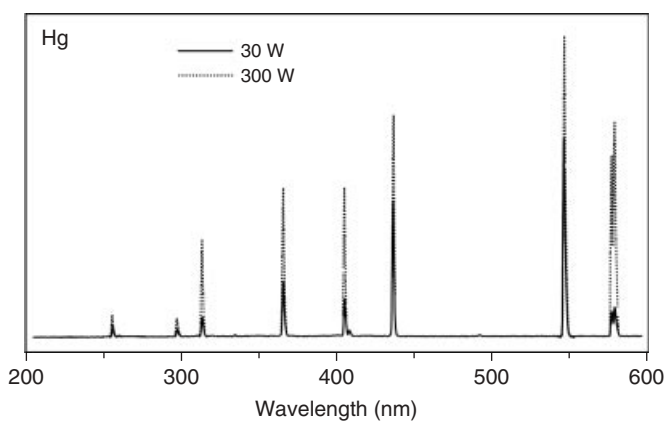


Figure 14.13 Emission spectra of a quartz Hg-EDL at 30 and 300 W output power in hexane [44].

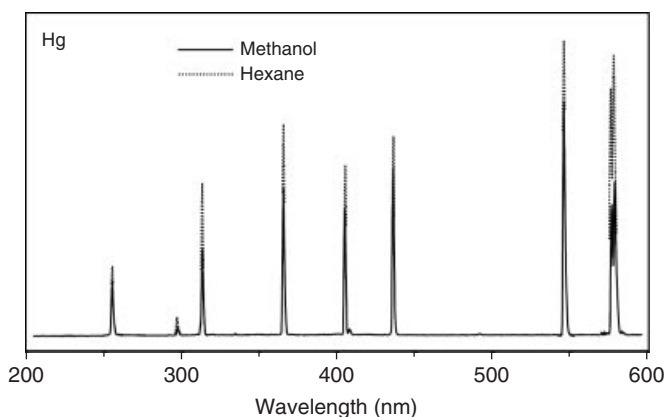


Figure 14.14 Emission spectra of a quartz Hg-EDL in methanol and hexane [44].

reaction conditions (temperature, solvent polarity) is essential for an efficient course of photochemical and photocatalytic processes in this experimental arrangement.

14.3

Microwave Photochemical and Photocatalytic Reactors

The photoreactor used for MW-assisted experiments is an essential tool for experimental work. Such equipment allows the simultaneous irradiation of compounds with both MW and UV/Vis radiation. Over the past decade, considerable experience has been obtained [94–96] in the construction of MW photochemical and photocatalytic reactors [12].

Various lamp configurations used in MW photoreactors are shown in Figure 14.15, where different arrangements of the lamps (external versus internal UV/Vis source) and their location in the MW field (outside versus inside) are presented. As a result, the batch and flow-through modes of seven fundamental types of MW photoreactors, **A1–A3** and **B1–B4**, were considered.

The simplest types of MW photoreactors are batch flasks (Figure 14.15, **A1**) or flow-through tubes (**B1**) located in the MW field, which are irradiated by a light beam from an external UV/Vis source (classical lamp or EDL). This type of equipment makes it possible to study the effects of MW radiation in the course of a photoreaction. However, for practical reasons, the batch photoreactors (**A2** and **A3**) with the EDL inside an MW oven have been widely applied.

The flow-through reactor types can be subdivided into an annular photoreactor (Figure 14.15, **B2**) with the EDL centered parallel to the axis of the reactor vessel; a cylindrical photoreactor (**B3**) with a coaxial radiation field that is generated by surrounding EDL; and a mixed flow-through photoreactor (**B4**) with an internal EDL inside the circulating reaction solution. Many MW photoreactors used in the laboratory are based on these designs.

Microwave photocatalytic reactors can also be divided into batch and flow-through modes; moreover, the type and variation of the photocatalyst (slurry versus thin film) needs to be considered further.

14.3.1

Performance in Batch Photoreactors

MW photochemistry and photocatalysis in batch reactors have been investigated over the past decade and can be implemented if external or internal lamps (classical UV lamp versus EDL) are used. Combination of given variables may lead to the following three types (**A1–A3**) of techniques for a batch setup in an MW field (Figure 14.15):

- 1) external classical UV lamp (**A1**)
- 2) internal EDL (**A2**)
- 3) internal EDL inside a double wall (**A3**).

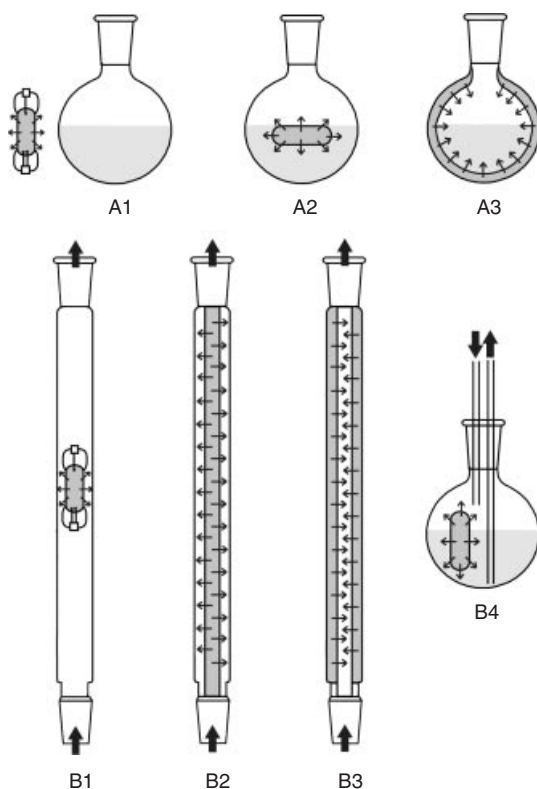


Figure 14.15 Cross-sectional view of various MW photoreactor types with different arrangement of the lamps: **(A1)** batch with external UV/Vis source (classical lamp); **(A2)** batch with an internal EDL; **(A3)** batch with EDL inside a double wall;

(B1) flow-through with internal UV/Vis source (classical lamp); **(B2)** annular flow-through with an internal EDL; **(B3)** cylindrical flow-through surrounded with EDL; and **(B4)** mixed flow-through with internal EDL.

14.3.1.1 Batch Photoreactors with External Classical UV Lamp (Type A1)

Chemat *et al.* [97] developed an original MW–UV combined reactor (Figure 14.16) based on a commercially available monomode MW reactor (Synthewave 402, Prolabo, France) and an external UV/Vis source (250 W medium-pressure Hg lamp). Also, Klán and co-workers [98] used this experimental arrangement to investigate photoreactions on alumina or silica gel surfaces.

Klán and Vavrik [99] used a modified MW oven with a quartz window for external UV irradiation (400 W high-pressure Hg lamp) to study a combined MW–UV–H₂O₂ remediation.

14.3.1.2 Batch Photoreactors with Internal EDL (Type A2)

Den Besten and Tracy [100] reported on an especially useful and convenient apparatus with an EDL (Figure 14.17) for the small-scale laboratory photolysis of

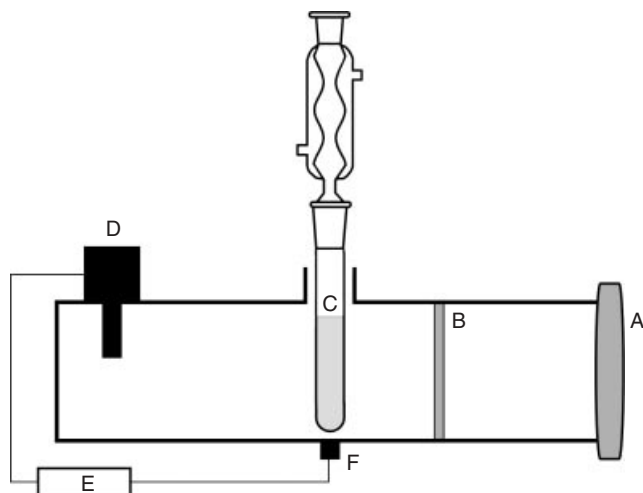


Figure 14.16 Reactor for MW photochemical experiments based on the Synthwave (Prolabo): (A) external UV/Vis lamp; (B) window of vision; (C) reaction mixture; (D) magnetron; (E) regulation; and (F) IR sensor. Adapted from [97].

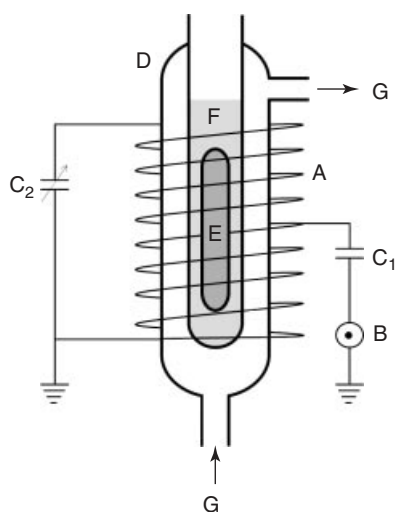


Figure 14.17 Apparatus with EDL for UV/Vis irradiation: (A) antenna; (B) transmitter; (C) capacitors; (D) jacketed flask; (E) EDL; (F) reaction mixture; and (G) circulating coolant. Adapted from [100].

organic compounds in solution or for irradiation of gases. In this arrangement, the EDL was placed in a reaction solution and operated by means of an external MW field from a radio- or MW-frequency transmitter. The quantum output of the lamp was controlled by changing the output of the transmitter or by using a dilute ionic

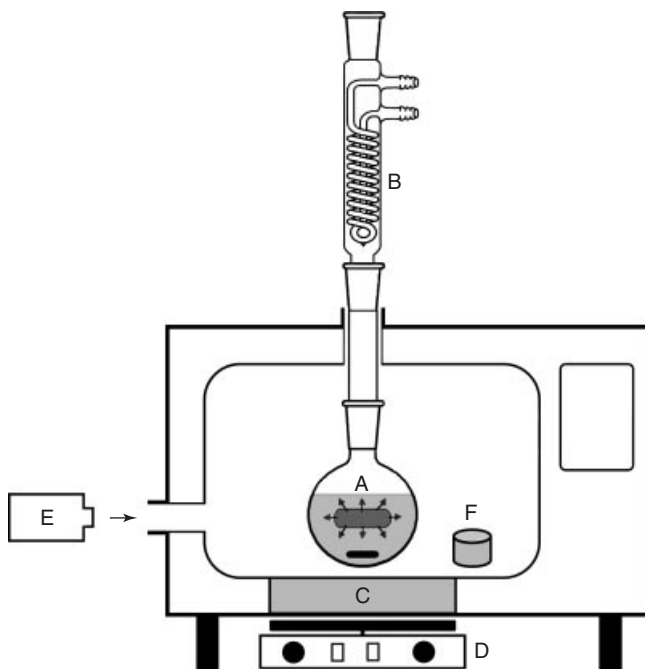


Figure 14.18 MW batch photochemical reactor: (A) reaction mixture with EDL and a magnetic stir bar; (B) Dimroth condenser; (C) aluminum plate; (D) magnetic stirrer; (E) fiber-optic spectral probe or external irradiation source; and (F) dummy load inside the oven cavity [101].

solution circulating through the cooling jacket. Placing the EDL in the solution was advantageous, because the full quantum output was used.

Čírkva and Hájek [101] reported on a simple MW photoreactor (Figure 14.18) with a quartz Hg-EDL developed for organic synthetic reactions. In a typical design, two holes were drilled into the walls of a domestic MW oven, one for a condenser tube in the oven top and the other in the side for a fiber-optic spectral probe or for external irradiation. Part of the oven bottom was replaced with an aluminum plate to permit magnetic stirring. A certain amount of an MW-absorbing solid material (dummy load: basic Al_2O_3 , molecular sieve, etc.) was inserted when a small quantity of a non- or poorly absorbing sample was used. The material removed excess MW power and prevented the magnetron from being destroyed by overheating.

Klán *et al.* [102] studied the use of Pyrex EDLs in an MW photoreactor to give the first systematic information about the technique, its scope, and its limitations. Table 14.2 depicts the most important advantages and disadvantages of EDL applications. In addition, Klán *et al.* [103] reported the first study of the temperature-dependent solvent effects on photoreactions in a MW field. Thus, this photochemical system was proposed as a reliable molecular photochemical thermometer.

Table 14.2 Advantages and disadvantages of EDLs in photo-applications [12].*Advantages*

Simultaneous UV/Vis and MW irradiation of the sample
 Simplicity of the experimental setup (use of a commercial MW oven, “wireless” EDL operation)
 Low cost of EDLs (easy methods of EDL preparation in the laboratory)
 Possibility of performing photo-experiments at high temperatures
 Good photo-efficiency: EDL is “inside” the sample
 Choice of the EDL material (Hg, S) might modify its spectral output

Disadvantages

Technical difficulties in performing experiments at temperatures below the solvent b.p.
 Intensity of EDLs depends strongly on given experimental conditions:
 (a) b.p., polarity, and transmittance of solvent
 (b) output and type of MW equipment
 (c) type and intensity of cooling

Müller *et al.* [104] carried out two temperature-sensitive photoreactions in high-temperature water (100–200 °C) in a pressurized vessel under MW heating (MicroSYNTH Labstation, Milestone) with a quartz Hg-EDL.

Čirkva *et al.* [105] studied the photohydrolysis of aqueous monochloroacetic acid (MCAA) to hydroxyacetic acid and HCl as a model reaction to evaluate a low-pressure batch MW photoreactor (Figure 14.19) equipped with quartz Hg-EDLs. Studies were carried out at relatively high MCAA concentration (0.1 mol l⁻¹), the desired temperature in the flow-through photoreactor was achieved by altering the total pressure of the system by a pump, and the photoreaction course was monitored by the pH change in the solution. This arrangement provided a unique possibility to study photochemical reactions under extreme thermal conditions (determination of the thermal dependence of a photoreaction) with the technical difficulties occurring when the MW photochemical experiments are performed at temperature below the boiling point of a solvent.

Horikoshi *et al.* [31] developed novel MW EDLs for wastewater treatment with AOPs using environment risk-free gases (e.g., xenon, nitrogen, helium, oxygen, hydrogen, and argon alone or mixtures thereof). The construction of the EDLs was optimized through examination of the light intensity of the emitted radiation in the UV/Vis region at controlled pressures and gas mixture ratios and to test whether the gases self-ignited on irradiation with MWs.

Florian and Knapp [66] developed a novel, MW-assisted, high-temperature UV digestion procedure for the accelerated decomposition of interfering dissolved organic carbon (DOC) prior to trace element analysis of liquid samples such as industrial/municipal wastewaters, body fluids, infusions, beverages, and sewage. The technique was based on a closed multiwave MW digestion device (Figure 14.20) equipped with a quartz pressure reaction vessel containing quartz Hg-, Cd-, and Zn-EDLs (254, 228, and 213 nm). To enhance the excitation efficiency (solution is



Figure 14.19 Low-pressure batch MW photoreactor [105].

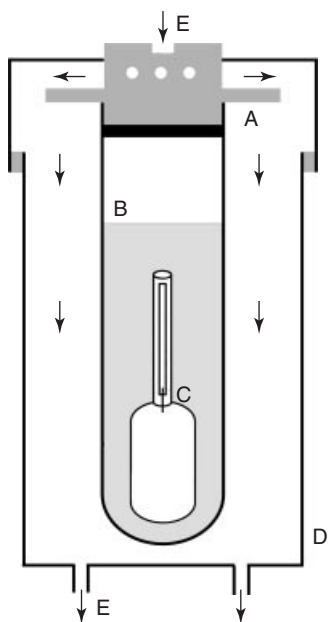


Figure 14.20 Simplified schematic diagram of a high-pressure digestion vessel with a quartz EDL: (A) plug and seal; (B) quartz pressure reaction vessel with sample solution; (C) EDL with an antenna; (D) PEEK vessel jacket with a screw-cap; and (E) air flow. Adapted from [66].

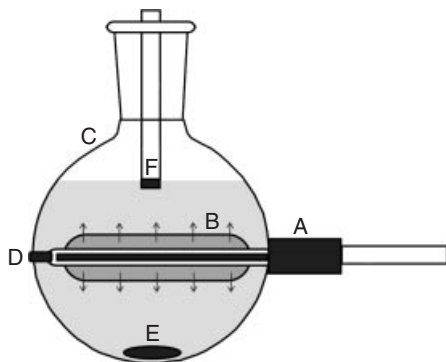


Figure 14.21 Immersed MW photoreactor with coaxial dipole antenna: (A) MW antenna with coaxial cable; (B) coaxial quartz EDL; (C) quartz flask with reaction mixture; (D) clamping post; (E) magnetic stir bar; and (F) spectral probe. Adapted from [106, 108].

shielding for the MW), an appropriate metal antenna (W wire and Mo foil of length 3 cm) was fixed on top of the EDL to focus the MW field.

Longo and co-workers [106–108] presented the characteristic features of a novel MW–UV photoreactor with a coaxial quartz Hg-EDL (Figure 14.21) using an immersed MW source as the coaxial MW antenna connected with flexible coaxial cable without the need to use an MW oven.

14.3.1.3 Batch Photoreactors with EDL Inside Double Wall (Type A3)

Howard *et al.* [109] employed a novel beaker-shaped quartz Hg-EDL in the breakdown of organophosphates into H_3PO_4 in preparation for colorimetric determination.

The efficiency of a new procedure based on an MW-activated quartz Hg-EDL photochemical reactor (Umex, Dresden, Germany) was evaluated by Peralta-Zamora and co-workers [110] (peroxide-assisted photodegradation of EDTA) and Grassi and co-workers [111] (digestion of natural waters).

Bergmann *et al.* [112] developed MW photoreactors (Umex) equipped with a quartz Hg-EDL for disinfecting drinking, waste, and feed waters with microorganism suspensions (*Bacillus subtilis*, *Saccharomyces cerevisiae*, and *Escherichia coli*). The experiments were performed in both batch and flow-through modes.

14.3.2

Performance in Flow-Through Photoreactors

MW photochemistry and photocatalysis in flow-through reactors have been investigated over the past decade and can be implemented if a classical UV lamp and an EDL are used. The combination of given variables may lead to the following four types (B1–B4) of techniques for a flow-through set-up in an MW field (Figure 14.15):

- 1) internal classical UV lamp (B1)
- 2) annular reactor with internal EDL (B2)
- 3) cylindrical reactor surrounded with EDL (B3)
- 4) mixed reactor with internal EDL (B4).

14.3.2.1 Flow-Through Photoreactors with Internal Classical UV Lamp (Type B1)

Han *et al.* [113] investigated the oxidative decomposition of aqueous phenol to hydroquinone, catechol, and consequently CO₂ and H₂O in an MW–UV–H₂O₂ system equipped with a classical low-pressure Hg lamp located at the center of the MW reactor. The authors claimed that MW radiation could considerably enhance the degradation of phenol even with suppression of thermal effects.

14.3.2.2 Annular Flow-Through Photoreactors with Internal EDL (Type B2)

Církva *et al.* [105] studied the photohydrolysis of aqueous MCAA to hydroxyacetic acid and HCl as a model reaction to evaluate a flow-through MW photoreactor (Figures 14.22 and 14.23) equipped with quartz Hg-EDLs. Studies were carried out at relatively high MCAA concentration (0.1 mol l⁻¹), the desired temperature in the flow-through photoreactor was achieved by adjustment of the pump flow speed, and the photoreaction course was monitored by the pH change in the solution. The effects of operating parameters (reaction temperature, quantum yield) on MCAA photohydrolysis were investigated. The MCAA conversion was optimized as a result of a trade-off between the thermal dependence of the photochemical quantum yield (which increases with increasing temperature) and the thermal dependence of the EDL light intensity of the 254 nm line [44] (which increases with decrease in temperature).

Longo and co-workers [106–108] also presented the characteristic features of a novel flow-through MW–UV photoreactor with a coaxial quartz Hg-EDL (analogous to Figure 14.21) using an immersed MW source as the coaxial MW antenna connected with a flexible coaxial cable without the need for an MW oven. The new equipment was tested in an MW–UV–H₂O₂ process for the photo-decoloration of Acid Orange 7 (AO7) azo dye.

Dong and co-workers [77] studied the photolysis of simulating a low concentration (25 mg m⁻³) of hydrogen sulfide malodorous gas under UV irradiation emitted by laboratory-made quartz Hg-I-EDLs (Hg, 185.0 and 253.7 nm; I₂, 178.3, 180.1, 183.0, 184.4, 187.6, 206.2, and 342 nm) in a flow-through gas MW–UV process.

14.3.2.3 Cylindrical Flow-Through Photoreactors Surrounded with EDL (Type B3)

Horikoshi *et al.* [114] proposed a novel double cylindrical photoreactor (Figure 14.24) equipped with a quartz Hg/Ne-EDL for photosensitization of an aqueous RhB solution.

Bergmann *et al.* [112] also developed a flow-through MW photoreactor (Umex) equipped with quartz Hg-EDL for disinfecting drinking, waste, and feed waters with microorganism suspensions (*Bacillus subtilis*, *Saccharomyces cerevisiae*, and *Escherichia coli*).

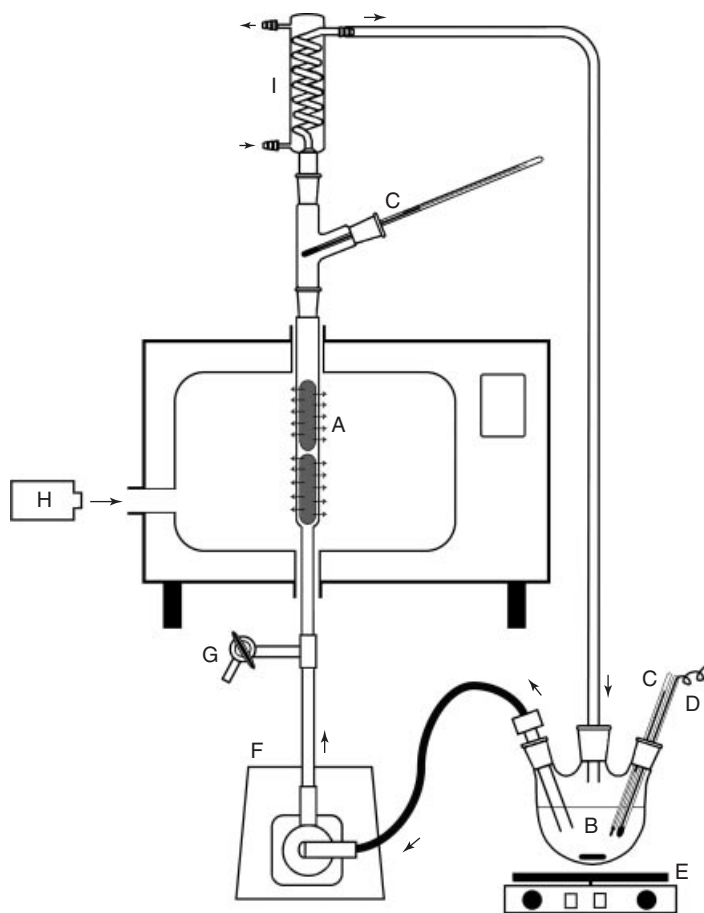


Figure 14.22 MW flow-through photochemical reactor: (A) reaction tube with EDLs; (B) glass reservoir with magnetic stir bar; (C) thermometer; (D) pH electrode; (E) magnetic stirrer; (F) PTFE diaphragm pump; (G) outlet; (H) spectrometer with a fiber-optic probe; and (I) cooling condenser [105].

14.3.2.4 Mixed Flow-Through Photoreactors with Internal EDL (Type B4)

Lu and co-workers [115] studied the degradation of aqueous 4-chlorophenol (4-CP) by direct photolysis in a mixed flow-through MW-assisted EDL system. The effect of the operating parameters was assessed and the degradation was enhanced in alkaline solution by increasing the irradiation EDL intensity, purging with oxygen, and adding H_2O_2 to the solution.

Zhang *et al.* [116, 117] studied the oxidative degradation of AO7 azo dye in the MW-UV- H_2O_2 process using a quartz Hg-EDL.

Horikoshi *et al.* [118] have examined the photooxidative destruction of bisphenol A and 2,4-D in aqueous media by using a VUV-transparent quartz W-triggered Hg-EDL (185 and 254 nm) under MW irradiation in a flow-through process. The



Figure 14.23 Flow-through MW photochemical reactor [105].

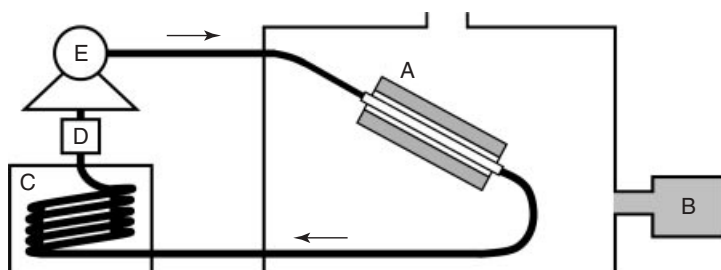


Figure 14.24 MW flow-through photochemical reactor: (A) cylindrical quartz Hg-EDL with sample solution; (B) magnetron; (C) cooling device; (D) thermometer; and (E) peristaltic pump. Adapted from [114].

185 nm radiation causes homolytic cleavage of the water molecule to produce H^\bullet and OH^\bullet radicals and molecular oxygen oxidation to give ozone and singlet oxygen as powerful oxidizing agents. This novel EDL provides an additional light source for AOPs without the need for a metal oxide photocatalyst.

Horikoshi and co-workers [32, 119] also developed a metallic condensing cone that concentrates MW radiation (equivalent to an optical lens) into an MW–UV photoreactor and used it as a part of the system to activate a quartz Hg-EDL (185 and 254 nm) in the oxidative treatment of wastewater. This approach to self-ignition of an EDL immersed in solution led to considerable energy savings.

An EDL immersed in aqueous solution presents some problems with regard to the continuity of UV/Vis light and most importantly self-ignition of a lamp by MW radiation [120]. This arises because when the EDL is used in aqueous media having a high dielectric loss factor, most of the MWs are absorbed by the dielectric medium. To compensate for this, self-ignition of the EDL requires significantly higher applied MW power levels. Nonetheless, there are methods by which the problem can be overcome. The first is to decrease the dielectric loss of the aqueous medium by heating it [121]. The second method involves the use of a tungsten trigger connected to the EDL [118] and the third technique includes a newly designed metallic condensing cone (equivalent to an optical lens) connected to a waveguide, which concentrates the MW radiation on to the sample [119]. The fourth method involves the use of a novel microwave discharge granulated electrodeless lamp (MDGEL, 5×10 mm) [120], and demonstrates some advantages of miniaturization, that is, greater surface area for irradiation, at low MW power levels. This system has been evaluated through the photoassisted defluorination of perfluoroalkanoic acids [120].

14.4

Interactions of UV/Vis and Microwave Radiation with Matter

Although MW chemistry [12] has already attracted widespread attention from the chemical community, considerably less information is available about the effect of MW radiation on photochemical reactions. Photochemistry is the study of the interaction of ultraviolet or visible radiation ($E = 600\text{--}170$ kJ mol⁻¹ at $\lambda = 200\text{--}700$ nm) with matter. The excess energy of electronically excited states significantly alters the reactivity of species – it corresponds, approximately, to typical reaction activation energies helping the molecules overcome activation barriers. The MW region of the electromagnetic spectrum, on the other hand, lies between infrared radiation and radiofrequencies. Its energy ($E = 1\text{--}100$ J mol⁻¹ at $\nu = 1\text{--}100$ GHz) is $\sim 3\text{--}6$ orders of magnitude lower than that of UV radiation (a typical MW kitchen oven operates at 2.45 GHz). MW heating is not identical with classical external heating, at least at the molecular level. Molecules with a permanent (or induced) dipole respond to an electromagnetic field by rotating, which results in friction with neighboring molecules (thus generating heat). Additional (secondary)

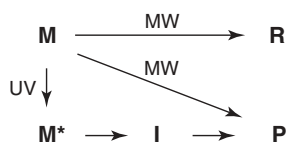


Figure 14.25 Simplified model of nonsynergic effects of UV and MW radiation on a chemical reaction.

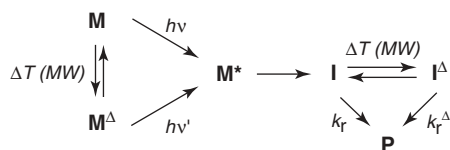


Figure 14.26 Simplified model of the synergic effect of UV and MW radiation on a chemical reaction, where Δ depicts “hot” molecules, and k_r and k_r^Δ are the rate constants of the processes leading eventually to the same product **P**.

effects of MWs include ionic conduction (ionic migration in the presence of an electric field) and spin alignment.

Simultaneous UV/Vis and MW irradiation of molecules, which does not necessarily cause any chemical change, might affect the course of a reaction by a variety of mechanisms in *each* step of the transformation. Of many possibilities, a simplified model describing two main distinct pathways has already been presented by Klán and Církva (Figure 14.25) [12]. The first route, more probable, is a photochemical reaction starting with a ground state molecule **M**, which is electronically excited to M^* , transformed into an intermediate (or a transition state) **I**, and finally a product **P**. Virtually every step may be complicated by a parallel MW-assisted reaction enabling a different chemical history. There is a theoretical possibility that MW radiation affects the electronically excited molecule M^* or a short-lived transition state. In such circumstances, the lifetime of the species should be long enough to provide a sufficient time for interaction with this low-frequency radiation. The second pathway becomes important when MWs initiate a “dark” chemical reaction (essentially through polar mechanisms), competitive with or exclusive to a photochemical pathway, yielding a different (**R**) or same (**P**) product. Figure 14.25 depicts a model in which MW and UV effects are easily distinguishable – it is assumed that there is no synergic effect during a single step of the transformation.

Let us, on the other hand, assume that the efficiency of a photoreaction is altered by MW induction [12]. In the example shown in Figure 14.26, MW heating affects the excitation energy of the starting ground state molecule. The individual effects of both types of electromagnetic radiation simultaneously influence a single chemical step in which the ground-state molecules **M** and M^Δ (an MW-heated molecule) are being excited. If, furthermore, the intermediates **I** and I^Δ react with different rate constants, the total observed rate constant k_{obs} of the reaction is proportional to the sum $k_{\text{obs}} \approx (\chi k_r + \chi^\Delta k_r^\Delta)$, where χ and χ^Δ represent the populations of **I** and I^Δ , respectively.

14.5

Microwave Photochemistry and Photocatalysis

The photochemical and photocatalytic systems can be divided into batch and flow-through types (A1–A3 and B1–B4) according to Figure 14.15. Examples of reactions investigated over the past decade by the MW photoexperiments are presented and summarized in Tables 14.3–14.6.

14.6

Applications

14.6.1

Analytical Applications

In addition to analytical applications in which MWs serve as a power source for the EDLs (Section 14.2.5.2), the first successful use of combined MW–UV irradiation for the efficient degradation of a variety of samples before a subsequent analytical application has been reported. Florian and Knapp [66] proposed a novel MW–UV, high-temperature, high-pressure digestion procedure for the decomposition of interfering DOC as a part of the trace element analysis of industrial and municipal wastewaters and other liquid samples.

Efficient decomposition of organophosphate compounds, with the aim of colorimetric phosphate determination, was achieved by Howard *et al.* in a novel beaker-shaped electrodeless MW–UV lamp [109]. Although no details of the organophosphate decomposition mechanism were presented, the authors suggested two possible pathways. In addition to a direct photodegradation, much of the decomposition resulted from the photochemical generation of hydroxyl and oxygen radicals from dissolved O₂ in the samples. The concentration of the OH radicals could be enhanced by the addition of hydrogen peroxide. In addition, Sodré *et al.* proposed a new procedure for the digestion of natural waters, based on a MW-activated photochemical reactor, in speciation studies of copper–humic substances [111].

14.6.2

Environmental Applications

Photodegradation [177] and MW thermolysis [178] of pollutants, toxic agents, and pathogens in wastewaters, often in combination with a solid catalyst (e.g., TiO₂), are two important methods for their removal. Results from environmentally relevant studies, in which a combined MW–UV technique [153, 179–185] was employed, have been published and the topic is also covered by several patents. Photochemical oxidation is a process in which a strong oxidizing reagent (ozone or hydrogen peroxide) is added to water in a UV-ionizing reactor, resulting in the generation of highly reactive hydroxyl radicals (OH[•]). The first-generation techniques used a commercial EDL (high pressure Hg–Xe lamps) immersed in

Table 14.3 Batch MW photochemical experiments.

Type	Lamp (envelope)	Reaction	Ref.	
A1	Class: Hg-MP	<i>o</i> -MeCO-C ₆ H ₄ -OCOPh (on bentonite) → <i>o</i> -HO-C ₆ H ₄ -COCH ₂ COPh	[97]	
	Class: Hg-HP	<i>p</i> -MeO-C ₆ H ₄ -NO ₂ + OH ⁻ → <i>p</i> -MeO-C ₆ H ₄ -OH + <i>p</i> -HO-C ₆ H ₄ -NO ₂ <i>p</i> -R-C ₆ H ₄ -COCH ₂ CH ₂ CHR' (R, R' = H, Me; Me, Me; H, C ₇ H ₁₅) (on alumina or silica gel) → <i>p</i> -R-C ₆ H ₄ -COMe + R'-CH=CH ₂ + cyclobutanols	[122] [98]	
A2	Hg-EDL (quartz)	Phenol, 4-chlorophenol, PCP, chlorobenzene, nitrobenzene + H ₂ O ₂	[99]	
		THF + CH ₂ =CH-C ₆ F ₁₃ → THF-CH ₂ CH ₂ -C ₆ F ₁₃	[101]	
		Valerophenone, 4-nitroanisole in high-temperature water	[104]	
		C ₆ H ₁₂ + C ₆ D ₁₂ → C ₆ H ₁₁ -C ₆ H ₁₁ + C ₆ H ₁₁ -C ₆ D ₁₁ + C ₆ D ₁₁ -C ₆ D ₁₁	[123]	
		C ₆ H ₁₂ + Me ₂ CHOH → C ₆ H ₁₁ -C ₆ H ₁₁ + C ₆ H ₁₁ -C(Me) ₂ OH + pinacole	[123]	
		4-Chlorophenol + H ₂ O ₂ → 4-chlorocatechol, hydroquinone, benzoquinone	[124, 125]	
		<i>o</i> - <i>tert</i> -Butylphenol → C-C dimers	[126]	
		<i>p</i> - <i>tert</i> -Butylphenol → C-C and C-O dimers + <i>o</i> - <i>tert</i> -butylphenol	[127]	
		1,4-Dihydropyridines + O ₂ → pyridines	[128]	
		Cl-CH ₂ CO ₂ H + H ₂ O → HO-CH ₂ CO ₂ H + HCl	[105]	
		Pentachlorophenol → tri- and tetrachlorophenols + chlorocatechols	[129]	
		Degradation of Acid Orange 7 azo dye in H ₂ O ₂	[106, 107]	
		Degradation of Active Brilliant Red X-3B (aqueous) on activated carbon	[130]	
		Hg-EDL (quartz) (Ar : Ne = 3 : 1)	<i>E</i> - <i>Z</i> photoisomerization of pent-2-en-4-yn-1-ol (HC≡C-CH=CH-CH ₂ OH)	[131]
		Hg-EDL (quartz, Pyrex)	Valerophenone → acetophenone + propene + cyclobutanols PhCOCH ₂ O ₂ CPh + (H-donor) → PhCOMe + PhCOOH PhCl + MeOH → PhOMe + HCl PhCOMe + Me ₂ CHOH → PhCH ₃ C(OH)-C(OH)PhCH ₃ + CH ₃ COCH ₃ PhOCOCH ₃ → <i>o</i> -HO-C ₆ H ₄ -COCH ₃ + <i>p</i> -HO-C ₆ H ₄ -COMe + PhOH	[48, 103]
		Hg-EDL (Pyrex)	Valerophenone → acetophenone + propene + cyclobutanols <i>p</i> -MeO-C ₆ H ₄ -NO ₂ + OH ⁻ → <i>p</i> -MeO-C ₆ H ₄ -OH + <i>p</i> -HO-C ₆ H ₄ -NO ₂ Degradation of Bromophenol Blue (aqueous) Degradation of atrazine (aqueous) with and without H ₂ O ₂	[102, 103] [122] [132] [133, 134]

Table 14.3 (continued.)

Type	Lamp (envelope)	Reaction	Ref.
A3	Cd-EDL (quartz, Mo/W)	Decomposition of insecticides (chlorfenvinphos, cypermethrin) using photo-Fenton ($\text{Fe}^{2+} + \text{H}_2\text{O}_2$)	[68]
		Digestion of skimmed milk, body fluids, infusions, beverages, sewage	[66]
		Digestion of the urban road dust (for determination of Pd)	[69]
		Digestion of serum, urine, milk, arsenobetaine solution	[70]
	I ₂ -EDL (Kr, quartz)	Decomposition of pyridine	[78]
		Decomposition of acetylferrocene, triphenyltin chloride, and dye CI Reactive Blue 13	[79]
	N ₂ /Ar-EDL (quartz)	Degradation of 2,4-dichlorophenoxyacetic acid (aqueous)	[31]
	Hg-EDL (quartz)	Polyphosphate/organophosphate ($\text{Na}_4\text{P}_2\text{O}_7$, 2-glycerophosphate, 4-nitrophenylphosphate, ATP) \rightarrow H_3PO_4	[109]
		Mineralization of $(\text{HO}_2\text{CCH}_2)_2\text{NCH}_2\text{CH}_2\text{N}(\text{CH}_2\text{CO}_2\text{H})_2$ in H_2O_2	[110]
		Decomposition of humic acid (aqueous) in H_2O_2	[111]
Disinfection of drinking/wastewaters with microorganism suspension		[112]	

water tanks. The lamps rapidly deteriorated, however, leading to poor production of hydroxyl radicals. The second-generation technique incorporated manual cleaning mechanisms and the use of a polymer coating (PTFE) on the quartz sleeve, additional oxidizers (ozone), and catalytic additives (TiO_2) to enhance the rate of OH radical production [186]. A novel UV-oxidation system used a highly efficient EDL combined with a simple coaxial flow-through reactor design [185]. In this reactor, a liquid containing contaminants (methyl *tert*-butyl ether, 2-propanol, or phenol) was pumped from the bottom and flowed vertically upwards through the reactor vessel against gravity. The mercury UV source was mounted above the reactor vessel and the radiation was directed downwards through the reactor vessel. An H_2O_2 solution was injected into the liquid being treated and thoroughly mixed by means of an in-line mixer just before the mixture entered the reactor vessel. It was found by Lipski *et al.* that photo-oxidation of humic acids causes changes in their absorption and luminescence properties that might be of a great importance for environmental photophysics and photochemistry [187]. Aqueous aerated alkaline solutions of the acids were irradiated with an Hg-EDL in a flow system and analyzed by means of fluorescence, absorption, and chemiluminescence techniques. Campanella *et al.* reported a minor but positive enhancement of the photocatalytic degradation efficiency of *o*- and *p*-CP aqueous solutions by MW heating [188]. The success of these model chemical systems offered an

Table 14.4 Flow-through MW photochemical experiments.

Type	Lamp (envelope)	Reaction	Ref.
B1	Class: Hg-LP	Decomposition of phenol (aqueous) in H ₂ O ₂ → hydroquinone + catechol	[113]
		Defluorination of CF ₃ CO ₂ H, C ₃ F ₇ CO ₂ H, and C ₇ F ₁₅ CO ₂ H (aqueous)	[120]
B2	Hg-EDL (quartz)	Cl-CH ₂ CO ₂ H + H ₂ O → HO-CH ₂ CO ₂ H + HCl	[105]
		Degradation of Acid Orange 7 azo dye in H ₂ O ₂	[106, 107]
		Photolysis of CS ₂	[80]
		Defluorination of CF ₃ CO ₂ H, C ₃ F ₇ CO ₂ H, and C ₇ F ₁₅ CO ₂ H (aqueous)	[120]
		H ₂ S (g) → SO ₄ ²⁻	[77, 135]
	Hg-EDL (quartz, W wire)	2,4-Dichlorophenoxyacetic acid, bisphenol-A	[118]
	I ₂ -EDL (Kr, quartz)	H ₂ S (g) → SO ₄ ²⁻	[77]
		Photolysis of CS ₂	[80]
		Degradation of butyl acetate	[64]
B3	Br ₂ -EDL (Kr, quartz)	Degradation of butyl acetate	[64]
	Hg-EDL (quartz)	Disinfection of drinking/wastewaters with microorganism suspension	[112]
B4	Hg/Ne-EDL (quartz)	Degradation of Rhodamine-B	[114]
		Degradation of 4-chlorophenol (aqueous)	[115]
	Hg-EDL (quartz)	Photoisomerization of <i>trans</i> - to <i>cis</i> -urocanic acid (aqueous)	[32]
		Degradation of Acid Orange 7 azo dye in H ₂ O ₂	[116, 117]
		Degradation of Reactive Brilliant Red X-3B dye(aqueous)	[136]
		Degradation of Reactive Red 195 dye (aqueous) in NaClO	[137]
	Hg-EDL (quartz, W)	Decomposition of bisphenol A and 2,4-dichlorophenoxyacetic acid (aqueous)	[118]
	Hg-EDL (quartz, MW cone)	Decomposition of 4-chlorophenol, 2,4-dichlorophenoxyacetic acid, bisphenol A	[119]
N ₂ -EDL (quartz, MW cone)	Photoisomerization of <i>trans</i> - to <i>cis</i> -urocanic acid (aqueous)	[32]	

extension to other environmentally interesting compounds, for example, sodium dodecylbenzenesulfonate or organophosphate pesticides. It has been suggested that MW-assisted photodegradation of pollutants may be of great interest in the future. Several other groups, such as Chemat *et al.* [97], Zheng *et al.* [189], Ai *et al.* [115], and Horikoshi and co-workers [144, 146, 161], have demonstrated improvements in degradative efficiency by coupling MW radiation to the photocatalytic degradation of various pollutants in aqueous solutions. Spherical and cylindrical EDLs have been used to remediate fluids, directly or by excitation of photocatalyst surfaces, which

Table 14.5 Batch MW photocatalytic experiments.

Type	Lamp (envelope)	Catalyst	Decomposition of	Ref.			
A1	Class: Hg-MP	Slurry TiO ₂	Rhodamine-B, benzoic acid,	[138–140]			
			Pyronin-B				
			Methylene Blue	[121]			
			5,5-Dimethyl-1-pyrroline <i>N</i> -oxide,	[141]			
			phenol				
			Bisphenol-A	[121, 142, 143]			
			Benzoic acid, phthalic acid,	[144]			
			<i>o</i> -formylbenzoic acid,				
			phthalaldehyde, succinic acid,				
			dimethyl phthalate, diethyl				
A2	Hg-EDL (quartz)	Slurry TiO ₂	phthalate, phenol				
			Methanol, ethanol, 1-propanol,	[145]			
			ethylene glycol, glycerin, acetone,				
			formic acid, acetic acid				
			2,4-Dichlorophenoxyacetic acid	[146]			
			Humic acid	[97]			
			4-Chlorophenol	[121, 147, 148]			
			Ethylene	[149]			
			A2	Hg-EDL (Pyrex)	Slurry TiO ₂ /C	Dimethyl phthalate	[150]
						Methylene Blue	[151]
Bromophenol	[132]						
Malachite Green	[152, 153]						
Crystal Violet	[153, 154]						
Phenol	[155]						
Rhodamine-B	[156]						
Atrazine	[157]						
A3	Cd-EDL (quartz)	Slurry TiO ₂				Pentachlorophenol	[129, 158]
						Rhodamine-B	[159]
			Dimethyl phthalate	[160]			
			Rhodamine-B	[108]			
			Cl-CH ₂ CO ₂ H, Rhodamine-B	[41, 43]			
			A3	Hg-EDL (Ne, quartz)	Slurry TiO ₂	Digestion of serum, urine, milk	[70]
						2,4-Dichlorophenoxyacetic acid	[161]

may be located on the lamps themselves, or on structures which are permeable by the fluids [166].

Noncatalytic remediation of aqueous solutions of various aromatic compounds by MW-assisted photolysis in the presence of hydrogen peroxide was studied by Klán and Vavrik [99]. The combined degradation effect of UV and MW radiation was found to be larger than the sum of isolated effects in all cases studied. It was concluded that such an overall efficiency increase is essentially based on the thermal

Table 14.6 Flow-through MW photocatalytic experiments.

Type	Lamp (envelope)	Catalyst	Decomposition of	Ref.
B1	Class: Hg-MP	Slurry TiO ₂	Rhodamine-B	[162]
			Phenol, <i>m</i> -cresol	[163]
B2	Hg-EDL (quartz)	Pellets TiO ₂	Acetaldehyde	[164]
	Hg-EDL (Pyrex)	Thin film TiO ₂	Cl-CH ₂ CO ₂ H	[165]
	EDL	Thin films	Fluid remediation	[166]
	Fluorescent bulb	Thin film TiO ₂ /ZrO ₂	Ethylene (g)	[149]
B3	Hg-EDL (Ne, quartz)	Slurry TiO ₂	Rhodamine-B	[114, 162]
			2,4-Dichlorophenoxyacetic acid	[146]
	Hg-EDL (quartz)	Slurry TiO ₂	Bromothymol Blue	[167]
		Thin film TiO ₂ on alumina balls	Propylene (g) Bromothymol Blue, Rhodamine-B, Methylene Blue	[168] [169, 170]
B4	Hg-EDL (quartz)	Slurry TiO ₂	4-Chlorophenol	[115, 124, 171]
			2-Chlorophenol,	[125, 172]
			4-chlorophenol,	
			2,4-dichlorophenol,	
			4-chloro-3-methylphenol,	
		2,4,6-trichlorophenol, pentachlorophenol		
	Slurry MnO ₂	Reactive Brilliant Red X-3B	[173, 174]	
		Acid Orange 7	[175]	
		Cationic Blue (X-GRL)	[176]	

enhancement of subsequent oxidation reactions of the primary photoreaction intermediates. Optimizations revealed that this effect is particularly significant in samples with a low concentration of H₂O₂; however, a larger excess of H₂O₂ was essential to complete the destruction in most experiments. The results from this work showed that the simultaneous MW–UV–H₂O₂ remediation technique could be an attractive alternative to conventional oxidation or photocatalytic degradation methods for the environmental remediation of polluted wastewater.

Sterilization techniques for intermittent or continuous destruction of pathogens in solid films or in organic and biological fluids, without significantly affecting the properties or physiological characteristics of the medium, are based on the biocidal synergism of UV and MW irradiation. UV radiation induces a chemical modification of DNA in bacteria (usually due to thymine dimerization). The first apparatus involved a commercial UV-emitting lamp with a separate power source inside the chamber of an MW oven and was used for simple sterilization of biological fluids [190]. An apparatus using an Hg-EDL for surface sterilization or disinfection of objects such as bottles, nipples, contact lenses, or food, was proposed by Le Vay [191] and Okuda and Atsumi [192]. A continuous sterilizing apparatus

[193, 194] has also been described for sterilizing bottle corks and textiles [195]. The sterilization effect of a MW-powered commercial UV lamp on the generation of active oxygen species to sterilize microorganisms was reported [196].

In addition, ozone treatment can be used in combination with UV exposure to sanitize or disinfect various substances [197–202]. Another application of EDLs (containing Hg, Cd/Ar, or Kr) for disinfecting aqueous solutions has recently been reported by Michael [203]. A photolysis and photocatalysis air pollution treatment system using an electrodeless UV lamp which treats a various types of air pollution using the high photochemical characteristics of electrodeless short-wavelength UV light has also been used [204]. Electrodeless excimer lamps have been applied to kill microbes [205].

14.6.3

Other Applications

Simultaneous application of UV and MW irradiation has found widespread use in industry. The techniques are based on conventional UV lamps or MW-powered electrodeless lamps [206]. Below we discuss a number of patents and papers that have described industrial MW-assisted photochemistry, such as treatment of wastewater, sterilization, and industrial photoinduced organic synthesis.

Photolithography is a technique for manufacturing semiconductor devices (i.e., transistors or integrated circuits). In the process, the pattern of an optical mask is imaged with UV radiation on to a semiconductor wafer coated with a UV-sensitive photoresist. The main goal is to reduce the size of the components and to increase their densities. Application of shorter wavelengths (190–260 nm) results in a greater depth of focus, that is, sharper printing. The first EDLs applied were made from a material known as *commercial water-containing natural quartz* [207]. It was found that the transmission of the envelope at vacuum UV wavelengths falls off sharply with time. The lamps developed later from water-free quartz [76] were much more transparent. Excimer lamps used for photoetching and microstructuring of the polymer surface have been developed for applications in standard MW ovens [62].

A photochemical apparatus for generating superoxide radicals ($O_2^{\bullet-}$) in an oxygen-saturated aqueous sodium formate solution by means of an EDL has been described [208]. An interesting method of initiating and promoting chemical processes by irradiation of starting gaseous materials in the electromagnetic field under a lower pressure was proposed by Lautenschläger [182]. EDLs (containing GaI₃, InI₃, or AlI₃) with a “blue” output are now often used for dental purposes or curing polymers. High-power MW lamps (H- and D-bulb, Fusion UV Curing System) were used for the polymerization of maleimide derivatives [209]. The very small size of the lamps makes them particularly useful for supplying light to an optical fiber or a light pipe [210]. Another example of MW photochemical treatment of solutions at different wavelengths was described by Moruzzi, which was found to be suitable for use in the promotion of photochemical reactions [211].

14.7

Future Trends

This chapter has presented a new method for carrying out photochemical and photocatalytic reactions with high efficiency in an MW field. The objective of MW photochemistry and photocatalysis is frequently, but not necessarily, connected to the EDL as a novel light source which generates UV/Vis radiation efficiently when placed into a MW field. The chapter focuses on the theory of an MW discharge in EDLs, the EDL construction, spectral characteristics, and performance, and the preparation of titania-coated films on EDLs. Novel MW photochemical and photocatalytic reactors with different arrangements of the lamps in batch and flow-through experimental setup have been described. The photochemical and photocatalytic reactions presented are summarized in several tables, and their detailed description will be the subject of an forthcoming review article.

We have discussed how the concept of MW photochemistry and photocatalysis is already an important issue in synthetic chemistry and material science. Although still in the early stages, detailed analysis of the past and recent literature confirms explicitly the usefulness of this method for chemical activation. The application of EDLs simplifies the technical procedures, especially in the field of organic photochemical and photocatalytic synthesis, environmental chemistry, and analysis.

Acknowledgments

The author is indebted to Professor Petr Klán (MU Brno, Czech Republic) who was engaged on the first aspects of this area and whose contributions have been significant. Thanks are due to the Grant Agency of the Czech Republic (104/07/1212) for funding this research. We are also grateful to Milestone srl (Italy) and Anton Paar GmbH (Austria) for their technical support.

References

1. Klán, P. and Wirz, J. (2009) *Photochemistry of Organic Compounds: From Concepts to Practice*, John Wiley & Sons, Ltd., Chichester.
2. Mattay, J. and Griesbeck, A. (1994) *Photochemical Key Steps in Organic Synthesis*, Wiley-VCH Verlag GmbH, Weinheim.
3. Griesbeck, A.G. and Mattay, J. (2005) *Synthetic Organic Photochemistry*, Marcel Dekker, New York.
4. Gedye, R., Smith, F., Westaway, K., Ali, H., Baldisera, L., Laberge, L., and Rousell, J. (1986) *Tetrahedron Lett.*, **27**, 279–282.
5. de la Hoz, A., Diaz-Ortiz, A., and Moreno, A. (2005) *Chem. Soc. Rev.*, **34**, 164–178.
6. Loupy, A. (ed.) (2006) *Microwaves in Organic Synthesis*, 2nd edn., Wiley-VCH Verlag GmbH, Weinheim.
7. Ahluwalia, V.K. and Varma, R.S. (2008) *Alternate Energy Processes in Chemical Synthesis. Microwave, Ultrasonic and Photo Activation*, Alpha Science International, Oxford.

8. Bogdal, D. (2005) *Microwave-Assisted Organic Synthesis. One Hundred Reaction Procedures*, Elsevier, Oxford.
9. Tierney, J.P. and Lidström, P. (2005) *Microwave Assisted Organic Synthesis*, Blackwell, Oxford.
10. Lidström, P., Tierney, J., Wathey, B., and Westman, J. (2001) *Tetrahedron*, **57**, 9225–9283.
11. Perreux, L. and Loupy, A. (2001) *Tetrahedron*, **57**, 9199–9223.
12. Klán, P. and Církva, V. (2006) in *Microwaves in Organic Synthesis*, 2nd edn., vol. 2 (ed. A. Loupy), Wiley-VCH Verlag GmbH, Weinheim, pp. 860–897.
13. (a) Chemat, F., Poux, M., DiMartino, J.L., and Berlan, J. (1996) *J. Microwave Power Electromagn. Energy*, **31**, 19–22; (b) Cravotto, G., Beggiato, M., Penoni, A., Palmisano, G., Tollari, S., Leveque, J.M., and Bonrath, W. (2005) *Tetrahedron Lett.*, **46**, 2267–2271.
14. Cutress, I.J., Marken, F., and Compton, R.G. (2009) *Electroanalysis*, **21**, 113–123.
15. (a) Církva, V. and Relich, S. (2011) *Curr. Org. Chem.*, **15**, 248–264; (b) Církva, V. and Relich, S. (2011) *Mini Rev. Org. Chem.*, **8**, 282–293.
16. (a) Církva, V. and Žabová, H. (2009) in *Handbook of Photocatalysts: Preparation, Structure and Applications* (ed. G.K. Castello), Nova Science Publishers, New York, Chapter 3, pp. 103–151; (b) Církva, V. and Žabová, H. (2010) *Photocatalysis on Titania-Coated Electrodeless Discharge Lamps*, Nova Science Publishers, New York.
17. (a) Horikoshi, S., Abe, M., and Serpone, N. (2009) *Photochem. Photobiol. Sci.*, **8**, 1087–1104; (b) Horikoshi, S. and Serpone, N. (2009) *J. Photochem. Photobiol. C*, **10**, 96–110; (c) Serpone, N., Horikoshi, S., and Emeline, A.V. (2010) *J. Photochem. Photobiol. C*, **11**, 114–131.
18. Remya, N. and Lin, J.G. (2011) *Chem. Eng. J.*, **166**, 797–813.
19. Fehsenfeld, F.C., Evenson, K.M., and Broida, H.P. (1965) *Rev. Sci. Instrum.*, **36**, 294–298.
20. Brown, S.C. (1966) *Introduction to Electrical Discharges in Gases*, John Wiley & Sons, Inc., New York.
21. Kazantsev, S.A., Khutorshchikov, V.I., Guthöhrlein, G.H., and Windholz, L. (1998) *Practical Spectroscopy of High-Frequency Discharges*, Plenum Press, New York.
22. Jackson, D.A. (1930) *Proc. R. Soc. London, Ser. A*, **128**, 508–512.
23. Meggers, W.F. and Westfall, F.O. (1950) *J. Res. Natl. Bur. Stand.*, **44**, 447–455.
24. Ganeev, A., Gavare, Z., Khutorshikov, V.I., Khutorshikov, S.V., Revalde, G., Skudra, A., Smirnova, G.M., and Stankov, N.R. (2003) *Spectrochim. Acta B*, **58**, 879–889.
25. Fridman, A. (2008) *Plasma Chemistry*, Cambridge University Press, New York.
26. Wertheimer, M.R., Fozza, A.C., and Holländer, A. (1999) *Nucl. Instrum. Methods Phys. Res. B*, **151**, 65–75.
27. Gleason, W.S. and Pertel, R. (1971) *Rev. Sci. Instrum.*, **42**, 1638–1643.
28. Haarsma, J.P.S., De Jong, G.J., and Agterdenbos, J. (1974) *Spectrochim. Acta B*, **29**, 1–18.
29. Sneddon, J., Browner, R.F., Keliher, P.N., Winefordner, J.D., Butcher, D.J., and Michel, R.G. (1989) *Prog. Anal. Spectrosc.*, **12**, 369–402.
30. Církva, V., Vlková, L., Relich, S., and Hájek, M. (2006) *J. Photochem. Photobiol. A*, **179**, 229–233.
31. Horikoshi, S., Kajitani, M., Sato, S., and Serpone, N. (2007) *J. Photochem. Photobiol. A*, **189**, 355–363.
32. Horikoshi, S., Sato, T., Sakamoto, K., Abe, M., and Serpone, N. (2011) *Photochem. Photobiol. Sci.*, **10**, 1239–1248.
33. Herrmann, J.M. (2005) *Top. Catal.*, **34**, 49–65.
34. Zhao, J. and Yang, X. (2003) *Build. Environ.*, **38**, 645–654.
35. Rajeshwar, K., Osugi, M.E., Chanmanee, W., Chenthamarakshan, C.R., Zaroni, M.V.B., Kajitvichyanukul, P., and Krishnan-Ayer, R. (2008) *J. Photochem. Photobiol. C*, **9**, 171–192.
36. Pérez-Hernandéz, R., Mendoza-Anaya, D., Fernández, M.E., and Gómez-Cortés, A. (2008) *J. Mol. Catal. A*, **281**, 200–206.

37. Yuan, Z.F., Li, B., Zhang, J.L., Xu, C., and Ke, J.J. (2006) *J. Sol–Gel Sci. Technol.*, **39**, 249–253.
38. Gelover, S., Mondragón, P., and Jiménez, A. (2004) *J. Photochem. Photobiol. A*, **165**, 241–246.
39. Kluson, P., Kacer, P., Cajthaml, T., and Kalaji, M. (2001) *J. Mater. Chem.*, **11**, 644–651.
40. Kluson, P., Kacer, P., Cajthaml, T., and Kalaji, M. (2003) *Chem. Biochem. Eng. Q.*, **17**, 183–190.
41. Církva, V., Žabová, H., and Hájek, M. (2008) *J. Photochem. Photobiol. A*, **198**, 13–17.
42. Kluson, P., Luskova, H., Cajthaml, T., and Solcova, O. (2006) *Thin Solid Films*, **495**, 18–23.
43. Žabová, H. and Církva, V. (2009) *J. Chem. Technol. Biotechnol.*, **84**, 1624–1630.
44. Müller, P., Klán, P., and Církva, V. (2003) *J. Photochem. Photobiol. A*, **158**, 1–5.
45. Müller, P., Klán, P., and Církva, V. (2005) *J. Photochem. Photobiol. A*, **171**, 51–57.
46. Phillips, R. (1983) *Sources and Applications of Ultraviolet Radiation*, Academic Press, London.
47. Stockwald, K. (2010) British Patent 2,472,486, filed 22 June 2010, issued 9 February 2011.
48. Literák, J. and Klán, P. (2000) *J. Photochem. Photobiol. A*, **137**, 29–35.
49. Dolan, J.T., Ury, M.G., Turner, B.P., Waymouth, J.F., and Wood, C.H. (1993) World Patent WO 93,21655, filed 13 April 1993, issued 28 October 1993.
50. Dolan, J.T., Turner, B.P., Ury, M.G., and Wood, C.H. (1996) US Patent 5,682,080, filed 30 October 1996, issued 28 October 1997.
51. Dolan, J.T., Ury, M.G., and Wood, C.H. (1993) US Patent 5,404,076, filed 3 June 1993, issued 4 April 1995.
52. Johnson, P.D., Dakin, J.T., and Anderson, J.M. (1987) US Patent 4,810,938, filed 1 October 1987, issued 7 March 1989.
53. Dakin, J.T., Berry, T., Duffy, M.E., and Russell, T.D. (1992) US Patent 5,363,015, filed 10 August 1992, issued 8 November 1994.
54. Shea, A.J., Feuersanger, A.E., Keeffe, W.M., and Struck, C.W. (1993) European Patent EP 06,03014, filed 20 December 1993, issued 22 June 1994.
55. Russell, T.D., Berry, T., Dakin, J.T., and Duffy, M.E. (1992) European Patent EP 05,42467, filed 4 November 1992, issued 19 May 1993.
56. Marshall, G.B. and West, T.S. (1970) *Anal. Chim. Acta*, **51**, 179–190.
57. Patel, B.M., Browner, R.F., and Winefordner, J.D. (1972) *Anal. Chem.*, **44**, 2272–2277.
58. Gilliard, R. and Hafidi, A. (2008) World Patent WO 2008, 048968, filed 16 October 2007, issued 24 April 2008.
59. Lapatovich, W.P., Gibbs, G.R., and Proud, J.M. (1984) US Patent 4,647,821, filed 4 September 1984, issued 3 March 1987.
60. Lapatovich, W.P., Gibbs, G.R., and Proud, J.M. (1982) US Patent 4,480,213, filed 26 July 1982, issued 30 October 1984.
61. Lapatovich, W.P. and Gibbs, G.R. (1982) US Patent 4,492,898, filed 26 July 1982, issued 8 January 1985.
62. Kogelschatz, U., Esrom, H., Zhang, J.Y., and Boyd, I.W. (2000) *Appl. Surf. Sci.*, **168**, 29–36.
63. Voronov, A. and Reber, S. (2007) World Patent WO 2007,128494, filed 3 May 2007, issued 15 November 2007.
64. Zhao, Y., Chen, Q., Hou, H., and He, J. (2011) *J. Hazard. Mater.*, **186**, 430–435.
65. Browner, R.F., Winefordner, J.D., and Glenn, T.H. (1972) US Patent 3,786,308, filed 6 March 1972, issued 15 January 1974.
66. Florian, D. and Knapp, G. (2001) *Anal. Chem.*, **73**, 1515–1520.
67. Ono, T. and Murayama, S. (1990) *Appl. Opt.*, **29**, 3934–3937.
68. Gromboni, C.F., Kamogawa, M.Y., Ferreira, A.G., Nóbrega, J.A., and Nogueira, A.R.A. (2007) *J. Photochem. Photobiol. A*, **185**, 32–37.
69. Limbeck, A. (2006) *Anal. Chim. Acta*, **575**, 114–119.
70. Matusiewicz, H. and Stanisiz, E. (2007) *Microchem. J.*, **86**, 9–16.

71. Yoshizawa, K., Kodama, H., Minowa, Y., Komura, H., and Ito, H. (1984) US Patent 4,498,029, filed 2 July 1984, issued 5 February 1985.
72. Hochi, A., Horii, S., Takeda, M., and Matsuoka, T. (1996) European Patent EP 07,62476, filed 23 August 1996, issued 12 March 1997.
73. Ury, M.G. and Wood, C.H. (1982) US Patent 4,859,906, filed 6 October 1982, issued 22 August 1989.
74. Haugsjaa, P.O., Nelson, W.F., Regan, R.J., and McNeil, W.H. (1975) US Patent 3,942,058, filed 21 April 1975, issued 2 March 1976.
75. Kramer, J.M., McNeil, W.H., and Haugsjaa, P.O. (1978) US Patent 4,206,387, filed 11 September 1978, issued 3 June 1980.
76. Mueller, P., Ury, M.G., and Wood, C.H. (1982) US Patent 4,501,993, filed 6 October 1982, issued 26 February 1985.
77. Xia, L.Y., Gu, D.H., Tan, J., Dong, W.B., and Hou, H.Q. (2008) *Chemosphere*, **71**, 1774–1780.
78. Bi, C., Ye, Z., Zhang, R., Gu, A., and Liu, L. (2011) *Fresenius Environ. Bull.*, **20**, 1320–1327.
79. Zhao, Y., He, J.C., Chen, Q., He, J., Hou, H.Q., and Zheng, Z. (2011) *Chem. Eng. J.*, **167**, 22–27.
80. Shao, C.L., Xia, L.Y., Gu, D.H., Zhang, R.X., and Hou, H.Q. (2007) *Environ. Sci.*, **28**, 1627–1631.
81. Nam, S.Y. (2008) World Patent WO 2009,011510, filed 8 July 2008, issued 22 January 2009.
82. Ukegawa, S. and Gallagher, C. (1998) US Patent 6,121,730, filed 5 June 1998, issued 19 September 2000.
83. Dakin, J.T. (1985) US Patent 4,783,615, filed 26 June 1985, issued 8 November 1988.
84. Witting, H.L. (1988) US Patent 4,890,042, filed 3 June 1988, issued 26 December 1989.
85. Kirkpatrick, D.A., Dolan, J.T., MacLennan, D.A., Turner, B.P., and Simpson, J.E. (2000) World Patent WO 00,70651, filed 28 April 2000, issued 23 November 2000.
86. Kamarehi, M., Levine, L., Ury, M.G., and Turner, B.P. (1994) US Patent 5,831,386, filed 17 October 1994, issued 3 November 1998.
87. Kirkpatrick, D.A., MacLennan, D.A., Petrova, T., Roberts, V.D., and Turner, B.P. (2002) World Patent WO 02,082501, filed 5 April 2002, issued 17 October 2002.
88. Didenko, A.N. and Shchukin, A.Y. (2010) *J. Commun. Technol. Electron.*, **55**, 359–374.
89. Dolan, J.T., Ury, M.G., Waymouth, J.F., and Wood, C.H. (1991) World Patent WO 92,08240, filed 24 October 1991, issued 14 May 1992.
90. Turner, B.P. (1994) US Patent 5,661,365, filed 17 October 1994, issued 16 August 1997.
91. Kim, H.S., Choi, J.S., Kang, H.J., Jeon, Y.S., and Jeon, H.S. (2000) European Patent EP 10,93152, filed 1 February 2000, issued 18 April 2001.
92. Kim, H.S., Choi, J.S., Kang, H.J., Jeon, Y.S., and Jeon, H.S. (2000) US Patent 6,633,111, filed 4 February 2000, issued 14 October 2003.
93. Relich, S., Církva, V., Vlková, L., and Hájek, M. (2006) Photochemistry in the microwave oven: preparation, evaluation and applications of electrodeless discharge lamps, in Proceedings of the 3rd International Conference on Microwave Chemistry, Brno, Czech Republic, 3–7 September 2006, p. PO-21.
94. Braun, A.M., Maurette, M.T., and Oliveros, E. (1991) *Photochemical Technology*, John Wiley & Sons, Ltd., Chichester.
95. De Lasa, H., Serrano, B., and Salaces, M. (2005) *Photocatalytic Reaction Engineering*, Springer, New York.
96. Oppenländer, T. (2003) *Photochemical Purification of Water and Air*, Wiley-VCH Verlag GmbH, Weinheim.
97. Chemat, S., Aouabed, A., Bartels, P.V., Esveld, D.C., and Chemat, F. (1999) *J. Microwave Power Electromagn. Energy*, **34**, 55–60.
98. Literák, J., Klán, P., Heger, D., and Loupy, A. (2003) *J. Photochem. Photobiol. A*, **154**, 155–159.
99. Klán, P. and Vavrik, M. (2006) *J. Photochem. Photobiol. A*, **177**, 24–33.

100. Den Besten, I.E. and Tracy, J.W. (1973) *J. Chem. Educ.*, **50**, 303.
101. Církva, V. and Hájek, M. (1999) *J. Photochem. Photobiol. A*, **123**, 21–23.
102. a) Klán, P., Literák, J., and Hájek, M. (1999) *J. Photochem. Photobiol. A*, **128**, 145–149; b) Klán, P., Hájek, M., and Církva, V. (2001) *J. Photochem. Photobiol. A*, **140**, 185–189.
103. Klán, P., Literák, J., and Relich, S. (2001) *J. Photochem. Photobiol. A*, **143**, 49–57.
104. Müller, P., Loupy, A., and Klán, P. (2005) *J. Photochem. Photobiol. A*, **172**, 146–150.
105. Církva, V., Relich, S., and Hájek, M. (2010) *J. Chem. Technol. Biotechnol.*, **85**, 185–191.
106. Ferrari, C., Longo, I., Tombari, E., and Bramanti, E. (2009) *J. Photochem. Photobiol. A*, **204**, 115–121.
107. Ferrari, C., Longo, I., Tombari, E., and Gasperini, L. (2010) *Int. J. Chem. React. Eng.*, **8**, A72, 10.
108. Longo, I. and Ricci, A.S. (2007) *J. Microwave Power Electromagn. Energy*, **41**, 4–19.
109. Howard, A.G., Labonne, L., and Rousay, E. (2001) *Analyst*, **126**, 141–143.
110. Kunz, A., Peralta-Zamora, P., and Durán, N. (2002) *Adv. Environ. Res.*, **7**, 197–202.
111. Sodrè, F.F., Peralta-Zamora, P.G., and Grassi, M.T. (2004) *Quim. Nova*, **27**, 695–700.
112. Bergmann, H., Iourtchouk, T., Schöps, K., and Bouzek, K. (2002) *Chem. Eng. J.*, **85**, 111–117.
113. Han, D.H., Cha, S.Y., and Yang, H.Y. (2004) *Water Res.*, **38**, 2782–2790.
114. Horikoshi, S., Hidaka, H., and Serpone, N. (2002) *J. Photochem. Photobiol. A*, **153**, 185–189.
115. Ai, Z., Yang, P., and Lu, X. (2004) *Fresenius Environ. Bull.*, **13**, 550–554.
116. Zhang, X., Wang, Y., Li, G., and Qu, J. (2006) *J. Hazard. Mater. B*, **134**, 183–189.
117. Zhang, X., Li, G., Wang, Y., and Qu, J. (2006) *J. Photochem. Photobiol. A*, **184**, 26–33.
118. Horikoshi, S., Miura, T., Kajitani, M., and Serpone, N. (2008) *Photochem. Photobiol. Sci.*, **7**, 303–310.
119. Horikoshi, S., Tsuchida, A., Sakai, H., Abe, M., Sato, S., and Serpone, N. (2009) *Photochem. Photobiol. Sci.*, **8**, 1618–1625.
120. Horikoshi, S., Tsuchida, A., Sakai, H., Abe, M., and Serpone, N. (2011) *J. Photochem. Photobiol. A*, **222**, 97–104.
121. Horikoshi, S., Sakai, F., Kajitani, M., Abe, M., and Serpone, N. (2009) *Chem. Phys. Lett.*, **470**, 304–307.
122. Klán, P., Růžička, R., Heger, D., Literák, J., Kulhánek, P., and Loupy, A. (2002) *Photochem. Photobiol. Sci.*, **1**, 1012–1016.
123. Nüchter, M., Ondruschka, B., Jungnickel, A., and Müller, U. (2000) *J. Phys. Org. Chem.*, **13**, 579–586.
124. Ai, Z., Yang, P., and Lu, X. (2005) *Chemosphere*, **60**, 824–827.
125. Wu, G., Yuan, S., Ai, Z., Xie, Q., Li, X., and Lu, X. (2005) *Fresenius Environ. Bull.*, **14**, 703–708.
126. Církva, V., Kurfürstová, J., Karban, J., and Hájek, M. (2004) *J. Photochem. Photobiol. A*, **168**, 197–204.
127. Církva, V., Kurfürstová, J., Karban, J., and Hájek, M. (2005) *J. Photochem. Photobiol. A*, **174**, 38–44.
128. Kormos, C.M., Hull, R.M., and Leadbeater, N.E. (2009) *Aust. J. Chem.*, **62**, 51–57.
129. Yang, S., Fu, H., Sun, C., and Gao, Z. (2009) *J. Hazard. Mater.*, **161**, 1281–1287.
130. Fu, J., Wen, T., Wang, Q., Zhang, X.W., Zeng, Q.F., An, S.Q., and Zhu, H.L. (2010) *Environ. Technol.*, **31**, 771–779.
131. Bonrath, W. and Ondruschka, B. (2008) World Patent WO 2009,080280, filed 18 December 2008, issued 2 July 2009.
132. Hong, J., Ta, N., Yang, S.Q., Liu, Y.Z., and Sun, C. (2007) *Desalination*, **214**, 62–69.
133. Ta, N., Hong, J., Liu, T., and Sun, C. (2006) *J. Hazard. Mater. B*, **138**, 187–194.
134. Chen, H., Bramanti, E., Longo, I., Onor, M., and Ferrari, C. (2011) *J. Hazard. Mater.*, **186**, 1808–1815.

135. Sun, X., Zhang, B., He, L., Hou, H.Q., and Zhang, R.X. (2010) *Chin. Chem. Lett.*, **21**, 968–972.
136. Cai, Y.J., Lin, L.N., Xia, D.S., Zeng, Q.F., and Zhu, H.L. (2011) *CLEAN*, **39**, 68–73.
137. Fu, J., Xu, Z., Li, Q.S., Chen, S., An, S.Q., Zeng, Q.F., and Zhu, H.L. (2010) *J. Environ. Sci.*, **22**, 512–518.
138. Horikoshi, S., Hidaka, H., and Serpone, N. (2002) *Environ. Sci. Technol.*, **36**, 1357–1366.
139. Horikoshi, S., Saitou, A., Hidaka, H., and Serpone, N. (2003) *Environ. Sci. Technol.*, **37**, 5813–5822.
140. Horikoshi, S., Kajitani, M., Hidaka, H., and Serpone, N. (2008) *J. Photochem. Photobiol. A*, **196**, 159–164.
141. Horikoshi, S., Hidaka, H., and Serpone, N. (2003) *Chem. Phys. Lett.*, **376**, 475–480.
142. Horikoshi, S., Tokunaga, A., Hidaka, H., and Serpone, N. (2004) *J. Photochem. Photobiol. A*, **162**, 33–40.
143. Horikoshi, S., Kajitani, M., and Serpone, N. (2007) *J. Photochem. Photobiol. A*, **188**, 1–4.
144. Horikoshi, S., Hojo, F., Hidaka, H., and Serpone, N. (2004) *Environ. Sci. Technol.*, **38**, 2198–2208.
145. Horikoshi, S., Abe, M., and Serpone, N. (2009) *Appl. Catal. B*, **89**, 284–287.
146. Horikoshi, S., Hidaka, H., and Serpone, N. (2003) *J. Photochem. Photobiol. A*, **159**, 289–300.
147. Horikoshi, S., Tokunaga, A., Watanabe, N., Hidaka, H., and Serpone, N. (2006) *J. Photochem. Photobiol. A*, **177**, 129–143.
148. Horikoshi, S., Sakai, F., Horikoshi, S., Abe, M., Emeline, A.V., and Serpone, N. (2009) *J. Phys. Chem. C*, **113**, 5649–5657.
149. Kataoka, S., Tompkins, D.T., Zeltner, W.A., and Anderson, M.A. (2002) *J. Photochem. Photobiol. A*, **148**, 323–330.
150. Liao, W. and Wang, P. (2009) *J. Braz. Chem. Soc.*, **20**, 866–872.
151. Hong, J., Sun, C., Yang, S.G., and Liu, Y.Z. (2006) *J. Hazard. Mater.*, **133**, 162–166.
152. Ju, Y., Yang, S., Ding, Y., Sun, C., Zhang, A., and Wang, L. (2008) *J. Phys. Chem.*, **112**, 11172–11177.
153. Ju, Y., Xu, Z., Liu, W., Zhang, Y., Chen, C., and Lin, B. (2010) Chinese Patent 101,885,530, filed 20 July 2010, issued 17 November 2010.
154. Ju, Y., Fang, J., Liu, X., Xu, Z., Ren, X., Sun, C., Yang, S., Ren, Q., Ding, Y., Yu, K., Wang, L., and Wei, Z. (2011) *J. Hazard. Mater.*, **185**, 1489–1498.
155. Liu, Y., Yang, S., Hong, J., and Sun, C. (2007) *J. Hazard. Mater.*, **142**, 208–215.
156. He, Z., Yang, S., Ju, Y., and Sun, C. (2009) *J. Environ. Sci.*, **21**, 268–272.
157. Gao, Z., Yang, S., Ta, N., and Sun, C. (2007) *J. Hazard. Mater.*, **145**, 424–430.
158. Gao, Z., Yang, S., Sun, C., and Hong, J. (2007) *Sep. Purif. Technol.*, **58**, 24–31.
159. Hea, Z., Sun, C., Yang, S., Ding, Y., He, H., and Wang, Z. (2009) *J. Hazard. Mater.*, **162**, 1477–1486.
160. Liao, W., Zheng, T., Wang, P., Tu, S., and Pan, W. (2010) *Environ. Eng. Sci.*, **27**, 1001–1007.
161. Horikoshi, S., Hidaka, H., and Serpone, N. (2004) *J. Photochem. Photobiol. A*, **161**, 221–225.
162. Horikoshi, S., Hidaka, H., and Serpone, N. (2002) *Environ. Sci. Technol.*, **36**, 5229–5237.
163. Karthikeyan, S. and Gopalakrishnan, A.N. (2011) *J. Sci. Ind. Res.*, **70**, 71–76.
164. Horikoshi, S., Kajitani, M., Horikoshi, N., Dillert, R., and Bahnemann, D.W. (2008) *J. Photochem. Photobiol. A*, **193**, 284–287.
165. Žabová, H., Církva, V., and Hájek, M. (2009) *J. Chem. Technol. Biotechnol.*, **84**, 1125–1129.
166. Obee, T.N., Hay, S.O., Sangiovanni, J.J., and Hertzberg, J.B. (2003) World Patent WO 03,094982, filed 10 April 2003, issued 20 November 2003.
167. Park, S.H., Kim, S.J., Seo, S.G., and Jung, S.C. (2010) *Nanoscale Res. Lett.*, **5**, 1627–1632.
168. Bae, Y.S. and Jung, S.C. (2010) *J. Ind. Eng. Chem.*, **16**, 947–951.
169. Jung, S.C. (2011) *Water Sci. Technol.*, **63**, 1491–1498.
170. Chae, J.S., Jung, D.S., Bae, Y.S., Park, S.H., Lee, D.J., Kim, S.J., Kim, B.H.,

- and Jung, S.C. (2010) *Korean J. Chem.*, **27**, 672–676.
171. Ai, Z., Yang, P., and Lu, X. (2005) *J. Hazard. Mater. B*, **124**, 147–152.
172. Li, F., Lu, X., Ai, Z., Yuan, S., and Mei, P. (2007) *Fresenius Environ. Bull.*, **16**, 1345–1350.
173. Zhang, X., Wang, Y., and Li, G. (2005) *J. Mol. Catal. A*, **237**, 199–205.
174. Zhang, X., Li, G., and Wang, Y. (2007) *Dyes Pigm.*, **74**, 536–544.
175. Zhang, X., Sun, D.D., Li, G., and Wang, Y. (2008) *J. Photochem. Photobiol. A*, **199**, 311–315.
176. Liu, R., Wang, H., Zhao, X., Xiao, S., and Qu, J. (2008) *Catal. Today*, **139**, 119–124.
177. Scott, J.P. and Ollis, D.F. (1995) *Environ. Prog.*, **14**, 88–103.
178. Windgasse, G. and Dauerman, L. (1992) *J. Microwave Power Electromagn. Energy*, **27**, 23–32.
179. Ulanov, I.M., Litvintsev, A.J., and Isupov, M.V. (2008) Russian Patent 2,390,498, filed 18 July 2008, issued 27 January 2010.
180. Jiang, L., Jiu, J., Luo, S., Ye, Z., and Zhou, Q. (2010) Chinese Patent 101,857,283, filed 18 June 2010, issued 13 October 2010.
181. Wang, P. and Liao, W. (2008) CN Patent 101,239,299, filed 19 March 2008, issued 13 August 2008.
182. Lautenschläger, W. (1989) European Patent EP 04,29814, filed 11 October 1989, issued 5 June 1991.
183. Rummmler, J.M. (1994) World Patent WO 94,25402, filed 28 April 1994, issued 10 November 1994.
184. Kurata, T. (1999) US Patent 6,007,323, filed 5 February 1999, issued 28 December 1999.
185. Oster, S.P. (2000) World Patent WO 00,55096, filed 16 March 2000, issued 21 September 2000.
186. Downey, W.F. Jr. (1993) US Patent 5,439,595, filed 25 August 1993, issued 8 August 1995.
187. Lipski, M., Slawinski, J., and Zych, D. (1999) *J. Fluoresc.*, **9**, 133–138.
188. Campanella, L., Cresti, R., Sammartino, M.P., and Visco, G. (1998) *Proc. SPIE*, **3534**, 105–113.
189. Zheng, Y., Li, D.Z., and Fu, X. (2001) *Chin. J. Catal.*, **22**, 165–167.
190. Boucher, R.M.G. (1973) US Patent 3,926,556, filed 30 May 1973, issued 16 December 1975.
191. Le Vay, T.C. (1991) US Patent 5,166,528, filed 4 October 1991, issued 24 November 1992.
192. Okuda, S. and Atsumi, K. (2002) European Patent EP 1,435,245, filed 15 October 2002, issued 7 July 2004.
193. Little, R.A.R. and Briggs, D. (1996) European Patent EP 07,72226, filed 5 November 1996, issued 7 May 1997.
194. Lucas, J. and Moruzzi, J.L. (1999) World Patent WO 00,32244, filed 23 November 1999, issued 8 June 2000.
195. Linn, H. (2000) German Patent 10008487, filed 24 February 2000, issued 6 September 2001.
196. Iwaguch, S., Matsumura, K., Tokuoka, Y., Wakui, S., and Kawashima, N. (2002) *Colloid Surf. B Biointerfaces*, **25**, 299–304.
197. Le Vay, T.C. and Rummel, J.A. (1996) World Patent WO 96,40298, filed 7 June 1996, issued 19 December 1996.
198. Hirsch, P. (1989) World Patent WO 89,09068, filed 30 March 1989, issued 5 October 1989.
199. Danilychev, V.A. (1996) US Patent 5,666,640, filed Apr. 2, 1996, issued Sep. 9, 1997.
200. Danilychev, V.A. (1997) US Patent 5,931,557, filed 3 September 1997, issued 3 August 1999.
201. Michael, J.D. (1999) US Patent 6,171,452, filed 24 June 1999, issued 9 January 2001.
202. Hur, B.U. and Park, Y.B. (2001) US Patent 6,762,414, filed 18 September 2001, issued 26 February 2004.
203. Michael, J.D. (1999) US Patent 6,162,406, filed 25 June 1999, issued 19 December 2000.
204. Rho, B.D. (2007) World Patent WO 2007,102701, filed 7 March 2007, issued 13 September 2007.
205. Song, W. (2011) Chinese Patent 102,097,282, filed 30 November 2010, issued 15 June 2011.

206. Spero, D.M., Eastlund, B.J., and Ury, M.G. (1973) US Patent 3,872,349, filed 22 August 1973, issued 18 March 1975.
207. Matthews, J.C., Ury, M.G., Wood, C.H., and Greenblatt, M. (1982) US Patent 4,532,427, filed 29 March 1982, issued 30 July 1985.
208. Holroyd, R.A. and Bielski, H.J. (1978) US Patent 4,199,419, filed 28 December 1978, issued 22 April 1980.
209. Andersson, H., Gedde, U.W., and Hult, A. (1996) *Macromolecules*, **29**, 1649–1654.
210. Lapatovich, W.P., Browne, J.M., Palmer, F.L., Buninger, A.B., and Chen, N.H. (1999) European Patent EP 09,62959, filed 20 April 1999, issued 8 December 1999.
211. Moruzzi, J.L. (2000) World Patent WO 01,09924, filed 26 July 2000, issued 8 February 2001.